Exact solution for a hydrogen atom in a magnetic field of arbitrary strength

Yu. P. Kravchenko and M. A. Liberman
Condensed Matter Theory Group, Department of Physics, Uppsala University, Box 530, S-751 21, Uppsala, Sweden
and P. Kapitsa Institute for Physical Problems, Russian Academy of Sciences, Vorob'evskoe sh. 2, Moscow, 117334, Russia

B. Johansson
Condensed Matter Theory Group, Department of Physics, Uppsala University, Box 530, S-751 21, Uppsala, Sweden
(Received 19 October 1995; revised manuscript received 25 January 1996)

An exact solution describing the quantum states of a hydrogen atom in a homogeneous magnetic field of arbitrary strength is obtained in the form of a power series in the radial variable with coefficients being polynomials in the sine of the polar angle. Energy levels and wave functions for the ground state and for several excited states are calculated exactly for the magnetic field varying in the range $0<B/(m^2e^3c/\hbar^3)\leqslant 4000$. [S1050-2947(96)11306-8]

PACS number(s): 32.60.+i, 31.15.−p, 02.30.Jr, 97.60.Jd

I. INTRODUCTION

The hydrogen atom in a uniform magnetic field remains one of the most fascinating unsolved problems in ''elementary'' nonrelativistic quantum mechanics. Despite the great progress in the development of quantum mechanics since the early days of this century, only several realistic quantum mechanical problems have been solved exactly until now. These problems are the energy spectrum of a hydrogen atom and of a hydrogen molecular ion, the energy levels of a harmonic oscillator giving the spectrum of a free electron in a uniform magnetic field, the so-called Landau levels, and the hydrogen atom in an external electric field.

The availability of the exact solution of a realistic physical problem is of great significance to theoretical physics. First, it provides a firm fundamental platform from which further developments can be pursued. If the solved problem is nonrelativistic, the exact solution can be used to accurately identify relativistic effects from experimental data. In the case of the hydrogen atom the exact solution provided the solid foundation for the development of the theory of atomic structure. Another important aspect of an exact solution is its importance from methodical and pedagogical points of view. For example, in elementary textbooks the exact solution for the hydrogen atom is used to explain the structure of heavier atoms and the principle of the Mendeleev Periodic Table.

A growing interest in the problem of the hydrogen atom in strong magnetic fields is motivated by its various applications in different branches of physics. The problem is important to astrophysics, solid state physics, and atomic spectroscopy.

The structure of matter on the surface of a neutron star where the magnetic field can be as high as 10^{12} G is strongly determined by the intensity of the field [1]. If atoms on the pulsar surface are strongly bound, forming a metal phase or chains with large binding energy, then the mechanism of the pulsar emission is due to the formation of the polar gap, and the pulsar magnetosphere is formed by the pair production in the polar gap [2]. On the contrary, if atoms on the surface of a neutron star are bound weakly, then the charged particles freely escape from the star, and the surface electric field is equal to zero [3]. Detailed calculations made in the assumption that the surface matter consists of a single sort of nuclei (the iron $Z=26$) showed that the cohesive energy of such a matter is not sufficient for supporting the first model [4]. However, there are indications that the bonding energy of heterogeneous molecules in strong magnetic fields is rather large [5], and there is a possibility that due to the accretion of hydrogen atoms onto the neutron star its surface may contain both light and heavy atoms. The cohesive energy of such a mixture can be large enough to support the finite electric field on the pulsar surface [6].

A quantitative understanding of problems related to the pulsar dynamics requires a good knowledge of the behavior of matter in superstrong magnetic fields, and the simplest one-electron hydrogen problem is invoked to be the cornerstone of this new atomic physics in the same manner as the field-free hydrogen atom is the basis for the whole theory of atomic structure.

Another very interesting and important astrophysical application of the magnetized hydrogen problem is the radiation from white dwarfs, which possess magnetic fields of the order of 10^7–10^8 G. Some spectral features of this radiation are identified with lines of magnetized hydrogen atoms [7], and complete knowledge of the excited hydrogen spectrum in the region of intermediate field strength, which is now limited to a small number of low-lying excited states [8], will be of significant importance to astrophysics.

The ''atomic'' scale of magnetic fields is available also in laboratory conditions for shallow impurities and hydrogenlike excitons in many semiconductors. Due to the small effective masses of the impurities and excitons and large dielectric constants of semiconducting materials, already a moderate magnetic field of the order of several tesla causes complete reconstruction of the energy spectrum and wave functions of the excitons [9]. In many semiconductors the photoexcitation spectrum of shallow impurities lies in the submillimeter band, which makes it possible to study transitions between excited donor states [10,11]. As has been shown recently, a strong magnetic field dramatically changes properties of the exciton gas in a semiconductor. If the field is so intense that the distance between the Landau levels

exceeds the binding energy of an exciton, the system of excitons becomes similar to a weakly nonideal Bose gas and is capable of forming the Bose-Einstein condensate and a superfluid state even at a relatively high temperature [12].

In the atomic spectroscopy the basic mechanism of the linear Zeeman effect responsible for shifting of atomic spectral lines by weak magnetic fields was essentially understood at the beginning of the century with the creation of quantum mechanics. The theoretical interest in the problem of the quadratic Zeeman effect has been initiated by experimentally observed remarkable regularities in the photoabsorption spectrum of barium [13]. In a moderate magnetic field the photoabsorption spectrum of the Rydberg orbitals changes its nature from typical Rydberg series to that of a series which is equally spaced and associated with the Landau resonances beyond the ionization threshold. In the intermediate region where the Coulomb and the magnetic interactions are comparable, the spectrum does not display those simple features. However, it was found [14] that the photoabsorption spectrum exhibits much more regular structure than expected.

The near crossings of energy levels and degeneracies which occur in the intermediate region have led to a suggestion that there exists an additional approximate constant of motion and, as a consequence, an approximate dynamical symmetry of the problem [15–19]. As is known, level crossings are possible only for terms of different symmetry [20]. The explanation of the nature of the regularities in the photoabsorption spectrum was a major step towards the understanding of the quadratic Zeeman effect and atomic diamagnetism in general.

The nonseparability of the Schrödinger equation for an electron in combined Coulomb and magnetic fields makes the theoretical description of the problem quite difficult, especially when the two field strengths are comparable. There is a principal difference between this situation and the case of an electron in combined Coulomb and external electric fields. These two problems, the Zeeman effect and the Stark effect for the hydrogen atom, are considered as the basis for understanding the behavior of atoms in external electromagnetic fields. The basic difference between the Stark effect and the Zeeman effect concerns the symmetry of the Hamiltonian and the integrability of the respective Schrödinger equations.

In the case of the Stark effect there is a full set of commuting operators, which are a projection of the orbital momentum $\hat{L}_z$ (z axis is chosen along the field) and the modified component of the Runge-Lenz vector [21]

$$\hat{A}_z = -\boldsymbol{z}\cdot\left[\frac{1}{2}(\hat{\mathbf{p}}\times\hat{\mathbf{L}}-\hat{\mathbf{L}}\times\hat{\mathbf{p}})-\frac{Ze\mathbf{r}}{r}+\mathbf{r}\times(\mathbf{r}\times\boldsymbol{z})\right],$$

where $\boldsymbol{z}$ is the unit vector. Thus, in this case there are two constants of motion and the symmetry of the problem is dynamical in nature. It is the direct product of groups O(2) $\times$O(2), which is the respective subgroup of the supersymmetry O(4) of the field-free Coulomb problem. An important consequence is that the Schrödinger equation is separable in parabolic coordinates, and the states are completely defined by a full set of quantum numbers, which are eigenvalues of the respective commuting operators [21]. Such a separation is tantamount to the exact solution in a sense that the energy and the wave function of any state can be computed with any precision.

In contrast, in the case of the Zeeman effect the presence of the external magnetic field completely destroys the supersymmetry of the pure Coulomb problem. Now there is neither a full set of the constants of motion nor ''good'' quantum numbers and the respective Schrödinger equation is not separable. This causes the main difficulties in the problem.

The hydrogen atom in a magnetic field has been tackled by many authors with the aid of various approaches ranging from the perturbation theory for the weak-field regime [22] to the adiabatic approximation for the opposite limit of very strong magnetic fields [23]. It was found that the perturbation series diverges already for small intensities of the field [24], and the perturbation analysis is not applicable for physically interesting field values. The adiabatic approximation is applicable only for extremely large values of the field, and its accuracy for strongly bound states is low. In the asymptotic limit $B\rightarrow\infty$ the adiabatic approximation gives for the binding energy of the ground state the value $\mathcal{E}=-\frac{1}{2}\ln^2 B$ (we use atomic units, see below). For all physically possible values of the field this estimate is about three times larger than the actual binding energy, and even for the hypothetical field $B\sim 10^{30}$ a.u. the adiabatic value is still 1.4 times larger than the true solution [25].

Among practical computational methods the leading role belongs to the Hartree-Fock-like technique [8], which is based on expansion of the wave function in terms of spherical harmonics or Landau orbitals and subsequent approximate solution of the obtained system of coupled integro-differential equations. The method seems to have not very good convergence in the intermediate field region and provides low precision for strongly bound states in the high-field domain [26]. However, it has allowed one to calculate the energies of low-lying states for the wide range of the magnetic field strength, as well as the splitting of the components of the Lyman, Balmer, Paschen, and Brackett lines of the hydrogen atom as functions of the magnetic field. In the work [27] the Hartree-Fock-like technique was used in combination with the scaling property of the Hamiltonian.

A powerful tool for establishing rigorous bounds on the energy values is the eigenvalue analysis technique [28–31]. However, the reported methods are applicable only to the lowest states or to highly excited states near the ionization threshold.

A standard method for the numerical solution of quantum-mechanical problems is the variational technique based on presentation of the wave function as a linear combination of basis functions and on subsequent minimization of the energy [32]. The most precise calculations of the lowest energy levels reported to date are variational calculations presented in [33]. It is necessary to mention calculations with Gaussian-type orbitals [34], which are very promising for investigation of molecules in the magnetic field.

Other reported techniques include fully numerical computations and semianalytical methods (e.g., [35,36]). Nevertheless, despite numerous investigations and the great progress which has been made so far, there is as yet no satisfactory solution of the problem, establishing a convincing theory of the quadratic Zeeman effects, which remains the major un-

solved problem in atomic physics. It is not yet possible to calculate with the necessary accuracy the energy levels of many excited states and the evolution of an arbitrary energy level as a function of the magnetic field strength from the zero-field limit to the regime where the magnetic and Coulomb fields are comparable.

In this paper we present the exact solution of the problem of the hydrogen atom in a uniform magnetic field. The solution is expressed as a power series in the radial variable and the sine of the polar angle. As an application of the obtained exact solution we present the energy levels for the ground state and for several excited states with accuracy up to 10^{-12} hartree.

The paper is organized as follows. In Sec. II, we formulate the problem and present the Schrödinger equation in atomic units. In Sec. III, the solution is derived in the form of a power series in the radial coordinate with the coefficients depending on the polar angle. The explicit form of these coefficients and appropriate recurrence relations are obtained and rigorously proven. In Sec. IV, we investigate the asymptotic behavior of the solution and transform the boundary conditions to a form which makes it possible to reduce the problem to the infinite set of algebraic equations. Different algebraic algorithms for solving the obtained set of equations, which are based on the truncation of the set at a finite index, are presented in Sec. V. Various aspects of the convergence of the solution and appropriate computational issues are dealt with in Sec. VI. In Sec. VII we present the exact calculated energy levels and wave functions for the ground state and for several excited states of the hydrogen atom in a uniform magnetic field.

II. FORMULATION OF THE PROBLEM

We do not take into account relativistic effects since for fields below 2.35×10^9 T they are negligible [33]. The effect of the finite proton mass can be accounted for by means of a constant energy shift [37,38], so in the present analysis the nucleus is assumed to be infinitely heavy, and its motion is neglected.

The motion of the atomic electron in the superposition of the Coulomb field of the nucleus and a uniform magnetic field is described by the Hamiltonian

$$\hat{H}=\frac{1}{2m_e}\left(\hat{\mathbf{p}}+\frac{e}{c}\mathbf{A}\right)^2-\frac{e^2}{r}, \tag{1}$$

where $\mathbf{A}$ is the vector potential and m_e is the electron mass. We introduce the spherical system of coordinates (r,θ,φ) and take the gauge of the vector potential as

$$\mathbf{A}=(0,\ 0,\ \tfrac{1}{2}Hr\sin\theta), \tag{2}$$

where H is the magnetic intensity. The Hamiltonian takes the form

$$\hat{H}=-\frac{\hbar^2}{2m_e}\nabla^2-i\hbar\frac{eH}{2m_ec}\frac{\partial}{\partial\varphi}+\frac{e^2H^2}{8m_ec^2}r^2\sin^2\theta-\frac{e^2}{r}. \tag{3}$$

If we choose the Bohr radius $a_0=\hbar^2/m_ee^2=5.3\times10^{-9}$ cm as the unit of length, one hartree $E_0=2\,\mathrm{Ry}=m_ee^4/\hbar^2=27.2$ eV as the unit of energy, and the value $H_0=m_e^2e^3c/\hbar^3=2.35\times10^9$ G as the unit of magnetic intensity, i.e., convert formulas from the Gaussian to the atomic system of units, then the Schrödinger equation $\hat{H}\Psi=E\Psi$ takes the following form:

$$\Psi_{rr}+\frac{2}{r}\Psi_r+\frac{1}{r^2}\Psi_{\theta\theta}+\frac{\cos\theta}{r^2\sin\theta}\Psi_\theta+\frac{1}{r^2\sin^2\theta}\Psi_{\varphi\varphi}+i\gamma\Psi_\varphi$$
$$-\tfrac{1}{4}\gamma^2r^2\sin^2\theta\Psi+\frac{2}{r}\Psi=-2E\Psi. \tag{4}$$

Here $\gamma=H/H_0$ denotes the dimensionless intensity of the magnetic field and subscripts r, θ, and φ denote partial derivatives.

The hydrogen atom in the magnetic field has two ''good'' quantum numbers, the magnetic quantum number m and the z-parity ν, so the total wave function Ψ may be presented as

$$\Psi(r,\theta,\varphi)=e^{im\varphi}(r\sin\theta)^{|m|}(r\cos\theta)^\nu\psi(r,\theta). \tag{5}$$

The Schrödinger equation (4) becomes

$$\psi_{rr}+2\frac{|m|+\nu+1}{r}\psi_r+\frac{1}{r^2}\psi_{\theta\theta}$$
$$+\frac{1}{r^2}[(2|m|+1)\cot\theta-2\nu\tan\theta]\psi_\theta$$
$$=\left[\frac{1}{4}\gamma^2r^2\sin^2\theta-\frac{2}{r}-(1+|m|)\gamma+2E_b\right]\psi. \tag{6}$$

Instead of the total energy E we have introduced a new parameter $E_b=(1+m+|m|)\gamma/2-E$, which coincides with the binding energy $\mathcal{E}=\gamma/2-E$ for $m\leq0$.

III. DERIVATION OF SOLUTION IN THE FORM OF A POWER SERIES

We look for the solution of the Schrödinger equation (6) in the form of a power series in r with coefficients depending on $t=\sin\theta$,

$$\psi(r,\theta)=\sum_{i=0}^{\infty}f_i(t)r^i. \tag{7}$$

Substituting expansion (7) into Eq. (6) and equating coefficients of equal powers of r, we obtain the following equation for the angle functions f_i:

$$(1-t^2)f_i''+\left[\frac{2|m|+1}{t}-2(|m|+\nu+1)t\right]f_i'$$
$$+i[i+2(|m|+\nu)+1]f_i$$
$$=\tfrac{1}{4}\gamma^2t^2f_{i-4}+[2E_b-\gamma(|m|+1)]f_{i-2}-2f_{i-1}. \tag{8}$$

This equation is formally valid for any values of i if we postulate that $f_i\equiv0$ for $i<0$. It is a nonhomogeneous linear

differential equation, and its solution may be represented as the sum of a particular integral $G_i(t)$ and any complementary function $F_i(t)$.

Let us first consider the corresponding homogeneous equation:

$$(1-t^2)F_i''+\left[\frac{2|m|+1}{t}-2(|m|+\nu+1)t\right]F_i' + i[i+2(|m|+\nu)+1]F_i=0. \tag{9}$$

We seek the solution of Eq. (9) in the form of a power series:

$$F_i(t)=\sum_{j=0}^{\infty} b_{i,j}t^j. \tag{10}$$

We substitute the series (10) into Eq. (9), equate coefficients of equal powers of t, and obtain the following recurrent relation for the coefficients $b_{i,j}$:

$$b_{i,j+2}=-\frac{(i-j)[i+j+2(|m|+\nu)+1]}{(j+2)(j+2|m|+2)}b_{i,j}. \tag{11}$$

This relation independently couples coefficients with even j and coefficients with odd j. Exactly one coefficient in each subset can be taken arbitrarily, since all other coefficients in the corresponding subset will be uniquely determined by this choice. Therefore, any solution of the homogeneous equation (9) may be represented as a linear combination of two base vectors, the first vector corresponds to the choice $b_{i,0}=1$, $b_{i,1}=0$, and the second one is determined by $b_{i,0}=0$, $b_{i,1}=1$.

The ratio $b_{i,j+2}/b_{i,j}$ tends to 1 as j goes to infinity, which means that at $t=1$ the function $F_i(t)$ becomes infinitely large, and the solution is not a physical one. However, this does not happen if the series (10) terminates at a finite j. As can be seen from the recurrent relation (11), it happens if $j=i$. Therefore, for even i a physically allowable solution of the homogeneous equation (9) involves only the first base vector $b_{i,0}=1$, $b_{i,1}=0$, while for odd i only the second base vector $b_{i,0}=0$, $b_{i,1}=1$ is acceptable. In both cases the function F_i is the product of an arbitrary constant C_i and a polynomial $H_i(t)=\Sigma_{j=0}^{i}h_{i,j}t^j$ with the lowest term equal to unity. The terms $b_{i,j}$ are given by

$$b_{i,j}=C_ih_{i,j}. \tag{12}$$

The function f_i assumes the following form:

$$f_i(t)=G_i(t)+C_iH_i(t). \tag{13}$$

Now we proceed to the search for the particular integral G_i of the nonhomogeneous equation (8). The fact that F_i is a polynomial of degree i leads to the assumption that the same is also true for the particular integral $G_i(t)$. The validity of this premise is rigorously proven below.

We look for a particular solution of f_i in the form of a power series:

$$G_i(t)=\sum_{j=0}^{\infty} a_{i,j}t^j. \tag{14}$$

As usual, we substitute this series into (8), equate coefficients of equal powers of t, and get the following recurrent relation for the coefficients $a_{i,j}$:

$$\begin{aligned}&(i-j)[i+j+2(|m|+\nu)+1]a_{i,j}\\&\quad+(j+2)(j+2|m|+2)a_{i,j+2}\\&\quad=\tfrac{1}{4}\gamma^2(a_{i-4,j-2}+C_{i-4}h_{i-4,j-2})\\&\qquad+[2E_b-\gamma(|m|+1)](a_{i-2,j}+C_{i-2}h_{i-2,j})\\&\qquad-2(a_{i-1,j}+C_{i-1}h_{i-1,j}).\end{aligned} \tag{15}$$

This expression is formally valid for any values of indices i and j if we assume that coefficients $a_{i,j}$ with $i<0$ or $j=-1,-2$ are equal to zero.

Now we shall prove the following statement. *Any physically allowable particular integral of Eq. (8) is a polynomial of degree i.*

Proof. We show by induction on i that

$$a_{i,j}=0, \quad j>i. \tag{16}$$

The induction hypothesis holds for $i=0$ since $f_0(t)=\psi(0,t)=\text{const}$ does not depend on t. We assume that it holds for $k<i$, that is, particular integrals G_k and, therefore, functions $f_k(t)$ are polynomials in t of degree k. If $j\geqslant i$, then the right-hand side of (15) is zero according to the induction hypothesis, and expression (15) is reduced to the following relationship:

$$a_{i,j+2}=\frac{(j-i)[i+j+2(|m|+\nu)+1]}{(j+2)(j+2|m|+2)}a_{i,j}. \tag{17}$$

As can be seen from this expression, $a_{i,i+2}$ and all the subsequent coefficients $a_{i,i+4}$, $a_{i,i+6}$, ... are equal to zero. If $j\to\infty$, then $a_{i,j+2}/a_{i,j}\to 1$, which means that if $a_{i,i+1}\neq 0$, then the particular integral tends to infinity as t tends to 1. Therefore, a physically acceptable particular integral must have $a_{i,j}=0$ for all $j>i$, proving the induction step.

If $j=i$, then Eq. (15) takes the form $0\times a_{i,i}=0$ and does not allow us to find the value of $a_{i,i}$. Therefore, this value may be taken arbitrarily. The most ''natural'' way is to put $a_{i,i}=0$.

The series (7) can now be rewritten in the form

$$\psi(r,\theta)=\sum_{i=0}^{\infty}\sum_{j=0}^{i} A_{i,j}r^i\sin^j\theta, \tag{18}$$

$$A_{i,j}=a_{i,j}+C_ih_{i,j}. \tag{19}$$

We have obtained two independent subsets of solutions: the first subset involves only even values of j and the second one contains only odd values of j. We should take into account, however, that any physical solution of the Schrödinger equation (6) must obey the following boundary condition on the axis:

$$\left.\frac{\partial\psi}{\partial\theta}\right|_{\theta=0}=0. \tag{20}$$

This means that if j is odd, then $A_{i,j}=0$, and the function ψ contains only even powers of the sine of the polar angle.

As a result, we have obtained the exact structure of the solution in the form of a power series in two variables, the radius and the sine of the polar angle:

$$\psi(r,\theta)=\sum_{k=0}^{\infty}\sin^{2k}\theta\sum_{i=2k}^{\infty}A_{i,2k}r^{i}, \tag{21}$$

$$A_{i,2k}=\begin{cases}a_{i,2k}+C_i h_{i,2k}, & i=2p,\\ a_{i,2k}, & i=2p+1.\end{cases} \tag{22}$$

The polynomials $H_i(t)$ differ from zero only for even i and are given by the formula

$$H_i(t)=\sum_{k=0}^{i/2}h_{i,2k}t^{2k}, \tag{23}$$

where $h_{i,0}=1$ and the other coefficients $h_{i,2k}$ are defined according to Eq. (11):

$$h_{i,2k+2}=-\frac{(i-2k)[i+2k+2(|m|+\nu)+1]}{4(k+1)(k+|m|+1)}h_{i,2k}. \tag{24}$$

The modified wave function $\psi(r,\theta)$ is completely determined by the infinite set of coefficients C_{2p}, $p=0,1,\ldots,\infty$. Since the Schrödinger equation is homogeneous and its solution is determined up to a normalizing factor, we may put an arbitrary nonzero coefficient from the set $\{C_{2p}\}$ to a certain nonzero value. If $\psi(0)\neq 0$, then we may choose $C_0=1$, otherwise the choice will be different.

The remaining coefficients $\{C_{2p}\}$ and the eigenvalue E_b must be determined from the boundary condition at infinity: $\psi(\infty,\theta)=0$. This condition, which is imposed on a one-dimensional interval, should be transformed to the infinite set of zero-dimensional conditions which must be equivalent to the set of unknowns. This step is described in the following section.

IV. BOUNDARY CONDITIONS

It is more convenient for the following analysis to rewrite the series (21), defining the modified wave function ψ, in the equivalent form:

$$\psi(r,\theta)=\sum_{k=0}^{\infty}\gamma^{k}(r\sin\theta)^{2k}g_{2k}(r). \tag{25}$$

Functions $g_{2k}(r)$ are related to the series (21) in the following way:

$$g_{2k}(r)=\frac{1}{\gamma^{k}}\sum_{i=2k}^{\infty}A_{i,2k}r^{i-2k}. \tag{26}$$

Substituting expansion (25) into the Schrödinger equation (6), we obtain the following chain of coupled differential equations:

$$\frac{1}{\gamma}g''_{2k}+2\frac{2k+|m|+\nu+1}{\gamma r}g'_{2k}+\left(\frac{2}{\gamma r}+1+|m|-\frac{2E_b}{\gamma}\right)g_{2k}$$
$$=\tfrac{1}{4}g_{2k-2}-4(k+1)(k+|m|+1)g_{2k+2}. \tag{27}$$

Equation (27) is valid for all non-negative values of k including $k=0$ if we postulate that $g_{-2}(r)\equiv 0$.

The wave function ψ tends to zero as r goes to infinity. The radial functions g_{2k} must behave in the same way. We assume that asymptotically their tendency to zero is determined by a decaying exponent which can be multiplied by a finite power of r:

$$g_{2k}(r)\sim B_{2k}r^{\eta_{2k}}\exp(-\kappa_{2k}r),\quad r\to\infty. \tag{28}$$

We substitute this expression into the coupling equation (27) and let the radius r tend to infinity at a fixed k:

$$\left(\frac{1}{\gamma}\kappa_{2k}^{2}+1+|m|-\frac{2E_b}{\gamma}\right)B_{2k}r^{\eta_{2k}}\exp(-\kappa_{2k}r)$$
$$+4(k+1)(k+|m|+1)B_{2k+2}r^{\eta_{2k+2}}\exp(-\kappa_{2k+2}r)$$
$$-\tfrac{1}{4}B_{2k-2}r^{\eta_{2k-2}}\exp(-\kappa_{2k-2}r)=0. \tag{29}$$

If $k=0$, then Eq. (29) becomes

$$r^{\eta_0-\eta_2}=-\frac{4\gamma(|m|+1)(B_2/B_0)}{\kappa_0^{2}+(|m|+1)\gamma-2E_b}e^{(\kappa_0-\kappa_2)r}. \tag{30}$$

This equality holds when r goes to infinity only if $\kappa_0=\kappa_2$ and $\eta_0=\eta_2$. In general, it can be proved by induction on k with the aid of Eq. (29) that $\kappa_{2k}=\kappa_0$ and $\eta_{2k}=\eta_0$ for all k. Therefore, all functions g_{2k} have the same asymptotic behavior, which is described by the following formula:

$$g_{2k}(r)\sim B_{2k}r^{\eta}\exp(-\kappa r),\quad r\to\infty. \tag{31}$$

For any nonzero strength of the magnetic field the electron motion in the region $\theta\approx 0$, $r\to\infty$ is perfectly described by the adiabatic approximation [9]. This fact allows us to get the values of η and κ:

$$\eta=\frac{1}{\sqrt{2E_b}},\quad \kappa=\sqrt{2E_b}. \tag{32}$$

The boundary conditions at infinity can now be written as

$$\lim_{r\to\infty}\frac{g'_{2k}(r)}{g_{2k}(r)}=-\kappa. \tag{33}$$

The set of boundary conditions (33) is equivalent to the set of coefficients $\{C_{2p}\}$. Since all the coefficients but one and the value of binding energy are not known, the obtained set of conditions (33) is equivalent to the set of unknowns.

V. THE ALGEBRAIC ALGORITHM

The set of boundary conditions (33) obtained in the preceding section is sufficient for the complete solution of the problem. However, in order to get a practical algorithm of the solution we need to reduce infinite sets of unknowns and conditions to finite sets and replace boundary conditions imposed at infinity with boundary conditions at a finite radius.

There are two methods of reducing the infinite set of unknowns to a finite set, which are based on terminating the set

of unknowns at a finite cutoff index and algebraic construction of a set of functions defined within a certain domain $0 \leqslant r \leqslant R < \infty$ and converging to a limiting function as the cutoff index increases. We discuss both of the techniques below.

A. The first method

The first method is based on truncating the set $\{C_{2p}\}$ at a finite index $p=l$. All C_{2p} with $p>l$ are assumed to be zeros. The set of boundary conditions is reduced in the same way, that is, we require only the first $l+1$ radial functions $g_0, g_2, \ldots, g_{2l}$ to satisfy the boundary conditions given by Eq. (33). The boundary conditions, in turn, are reduced to the conditions imposed at a finite radius $r=R$:

$$\frac{g'_{2k}(R)}{g_{2k}(R)} = -\kappa. \tag{34}$$

The joining radius R must be chosen so that the first $l+1$ radial functions monotonically tend to zero on $[R,\infty]$.

In order to simplify the following discussion we introduce the concept of the ''trace'' of a coefficient C_{2n}. Let us choose the following values of C_{2p}:

$$C_{2p} = \begin{cases} 1, & p=n \\ 0, & p \neq n. \end{cases} \tag{35}$$

We compute all $a_{i,j}$ and $b_{i,j}$, according to Eqs. (12), (15), and (24), and designate obtained terms via $T^n_{i,j}$:

$$T^n_{i,j} = a_{i,j} + b_{i,j} = \begin{cases} 0, & i<2n \\ h_{2n,j}, & i=2n \\ a_{i,j}, & i>2n. \end{cases} \tag{36}$$

We define the resulting function $\phi_n(r,t)$ as the ''trace'' of the coefficient C_{2n}:

$$\phi_n(r,t) = \sum_{k=0}^{\infty} \sum_{i=2k}^{\infty} T^n_{i,2k} r^i t^{2k}. \tag{37}$$

The wave function ψ is the sum of products of coefficients C_{2p} and their ''traces'':

$$\psi(r,t) = \sum_{p=0}^{\infty} C_{2p} \phi_p(r,t). \tag{38}$$

The ''trace'' can also be represented as a sum of radial functions in a form similar to Eq. (25):

$$\phi_n(r,t) = \sum_{k=0}^{\infty} \gamma^k (rt)^{2k} q^n_{2k}(r). \tag{39}$$

The radial functions q^n_{2k} and their derivatives are given by

$$q^n_{2k}(r) = \frac{1}{\gamma^k} \sum_{i=2k}^{\infty} T^n_{i,2k} r^{i-2k}, \tag{40a}$$

$$\frac{d}{dr} q^n_{2k}(r) = \frac{1}{\gamma^k} \sum_{i=2k+1}^{\infty} (i-2k) T^n_{i,2k} r^{i-2k-1}. \tag{40b}$$

The radial functions $g_{2k}(r)$ are linear combinations of the functions q^n_{2k}:

$$g_{2k}(r) = \sum_{p=0}^{\infty} C_{2p} q^p_{2k}(r), \tag{41a}$$

$$g'_{2k}(r) = \sum_{p=0}^{\infty} C_{2p} \frac{d}{dr} q^p_{2k}(r). \tag{41b}$$

The boundary conditions (34) take the form

$$\sum_{p=0}^{\infty} C_{2p} \left[\frac{d}{dr} q^p_{2k}(R) + \kappa q^p_{2k}(R) \right] = 0. \tag{42}$$

Since we consider the truncated set of coefficients C_{2p}, the summation in Eq. (38) must extend only to l instead of infinity, and the exact function ψ is replaced with a reduced function $\widetilde{\psi}_{l,R}$:

$$\widetilde{\psi}_{l,R}(r,t) = \sum_{p=0}^{l} C_{2p} \phi_p(r,t)$$

$$= \sum_{k=0}^{\infty} \gamma^k (rt)^{2k} \widetilde{g}_{2k}(r), \tag{43}$$

$$\widetilde{g}_{2k}(r) = \sum_{p=0}^{l} C_{2p} q^p_{2k}(r). \tag{44}$$

The index R in the definition of $\widetilde{\psi}_{l,R}$ symbolizes that this function satisfies boundary conditions imposed on $l+1$ radial functions $\widetilde{g}_{2k}(r)$ at $r=R$:

$$\widetilde{g}\,'_{2k}(R) + \kappa \widetilde{g}_{2k}(R) = 0, \quad k = 0,1,\ldots,l. \tag{45}$$

Now we need to find the coefficients C_{2p}, $p=0,1,\ldots,l$, and the value of E_b. At least one of the coefficients C_{2p} in the solution will differ from zero. Let us denote the index of such a coefficient via d: $C_{2d} \neq 0$. Since the Schrödinger equation is homogeneous and its solution can be multiplied by a normalizing factor, we may choose $C_{2d}=1$. As a result, we have $l+1$ unknowns: the value of E_b and $\{C_{2p}: 0 \leqslant p \leqslant l,\ p \neq d\}$, which must satisfy $l+1$ equations (45). The coefficients C_{2p} enter Eq. (45) in a linear way and can be found directly as the solution of a system of l linear equations.

In order to find the values of $q^p_{2k}(R)$ and $(dq^p_{2k}/dr)(R)$ one needs to compute infinite sums in Eq. (40). However, asymptotically (as $i \to \infty$) the values $T^n_{i,2k} R^i$ converge to zero very fast (see Sec. VI A), and the values of $q^p_{2k}(R)$ and $(dq^p_{2k}/dr)(R)$ may be calculated with any desired precision by terminating the summation in Eq. (40) at a finite i.

One of the possible algorithms of finding the unknowns is to solve the system (45) with $k=1,2,\ldots,l$ with respect to the l unknown coefficients C_{2p}, $p \neq d$, at a fixed value of E_b, and to substitute the obtained values of C_{2p} into Eq. (45) at $k=0$. If E_b is not an exact solution, then the left-hand side of (45), which we designate here as

$$\Delta(E_b) = \widetilde{g}\,'_0(R) + \kappa \widetilde{g}_0(R) \tag{46}$$

and which nonlinearly depends on E_b, will differ from zero. Instead of the system of $l+1$ equations (45) we now have a single nonlinear equation $\Delta(E_b)=0$, which can be solved by an iterative method with arbitrarily high precision. Its roots E_b define energy levels in the considered l,R approximation.

The general character of the energy spectrum within each m,ν subspace corresponds to a typical atomic spectrum of bound states. The largest in magnitude root E_b corresponds to the ground state, other roots corresponding to various excited states lie in the interval between zero energy and the ground energy. The structure of the spectrum, especially in the region of intermediate field strength, is very complicated. Although for low-lying states a field-free-like classification was developed [22] and widely adopted (see [8]), it seems difficult to apply that scheme consistently for higher states. In order to avoid any ambiguity we shall label the roots successively by the index S, starting from the ground state $(S=0)$ and going to excited states. Since the roots depend also on l and R, we denote them as $(\tilde{E}_b^S)_{l,R}$.

At a fixed R the obtained solutions $(\tilde{E}_b^S)_{l,R}$ and $\tilde{\psi}_{l,R}$ converge to their limits as the number of coefficients l increases:

$$\lim_{l\to\infty}(\tilde{E}_b^S)_{l,R}=(E_b^S)_R, \tag{47}$$

$$\lim_{l\to\infty}\tilde{\psi}_{l,R}(r,t)=\Phi_R(r,t). \tag{48}$$

As the radius R increases, the value $(E_b^S)_R$ converges to the exact energy level E_b^S, and at any given point (r,t) the function $\Phi_R(r,t)$ converges to the exact solution $\psi(r,t)$:

$$\lim_{R\to\infty}(E_b^S)_R=E_b^S, \tag{49}$$

$$\lim_{R\to\infty}\Phi_R(r,t)=\psi(r,t). \tag{50}$$

The character of convergence makes it possible to control the upper bound of discrepancy between the value $(\tilde{E}_b^S)_{l,R}$ and the exact value E_b^S. This can be achieved by comparing results obtained with different values of l and R and is discussed in detail in Sec. VI, along with some aspects of the computational technique.

As a result, the outlined algorithm allows straightforward algebraic computation of energy levels and wave functions of the hydrogen in a magnetic field with any desired precision. However, this technique is not the only one available, and another method of reducing the infinite set of unknowns to a finite set which is described below solves the problem in a much more efficient way, involving a considerably smaller amount of arithmetical operations, while keeping all the advantages of the above scheme.

B. The second method

Instead of truncating the set of coefficients $\{C_{2p}\}$ we can terminate the infinite set of radial functions given by Eqs. (25) and (26). We take a finite l and assume that for $k>l$ radial functions $g_{2k}(r)$ are identically equal to zero:

$$g_{2k}(r)\equiv 0, \quad k>l. \tag{51}$$

In terms of coefficients C_{2p} this method of truncation means that instead of putting coefficients C_{2p} with $p>l$ to zero we choose them in such a way that

$$a_{2p,2l+2}+C_{2p}h_{2p,2l+2}=0. \tag{52}$$

The boundary conditions are reduced to a finite radius R according to Eq. (34), as was done in the first method.

To facilitate the further discussion we define the ''l-trace'' of a coefficient C_{2n}. We choose the following values of coefficients C_{2p}:

$$C_{2p}=\begin{cases}1, & p=n\leqslant l\\ 0, & p\neq n, \quad p\leqslant l,\end{cases} \tag{53}$$

and compute values $a_{i,j}$ and $b_{i,j}$ with $j\leqslant 2l$, following Eqs. (12) and (15). In contrast to the first method, all $a_{i,j}$ with $j>2l$ are put to zeros, which means that values C_{2p} with $p>l$ are taken implicitly in accordance with Eq. (52). We denote the obtained terms via $(\mathsf{T}_l^n)_{i,j}$:

$$(\mathsf{T}_l^n)_{i,j}=a_{i,j}+b_{i,j}=\begin{cases}0, & i<2n \quad \text{or} \quad j>2l\\ h_{2n,j}, & i=2n\\ a_{i,j}, & i>2n.\end{cases} \tag{54}$$

The resulting function $\omega_{l,n}(r,t)$ is the ''l-trace'' of the coefficient C_{2n}:

$$\omega_{l,n}(r,t)=\sum_{k=0}^{l}\sum_{i=2k}^{\infty}(\mathsf{T}_l^n)_{i,2k}r^i t^{2k}. \tag{55}$$

The wave function $\psi(r,t)$ is the limit of the sum of $l+1$ products of coefficients C_{2p} by their l-traces as l goes to infinity:

$$\psi(r,t)=\lim_{l\to\infty}\sum_{p=0}^{l}C_{2p}\omega_{l,p}(r,t) \tag{56a}$$

$$=\lim_{l\to\infty}\sum_{k=0}^{l}\gamma^k(rt)^{2k}w_{l,2k}(r), \tag{56b}$$

where the radial functions $w_{l,2k}(r)$ are

$$w_{l,2k}(r)=\frac{1}{\gamma^k}\sum_{p=0}^{l}C_{2p}\sum_{i=2k}^{\infty}(\mathsf{T}_l^p)_{i,2k}r^{i-2k}. \tag{57}$$

Termination of the set of radial functions results in removing the limit sign from Eq. (56) and replacing the exact function $\psi(r,t)$ with a reduced function $\hat{\psi}_{l,R}$:

$$\hat{\psi}_{l,R}(r,t)=\sum_{p=0}^{l}C_{2p}\omega_{l,p}(r,t)=\sum_{k=0}^{l}\gamma^k(rt)^{2k}w_{l,2k}(r). \tag{58}$$

The reduced function $\hat{\psi}_{l,R}$ must satisfy $l+1$ boundary conditions imposed at a finite radius R:

$$w'_{l,2k}(R)+\kappa w_{l,2k}(R)=0, \quad k=0,1,\ldots,l. \tag{59}$$

Unknown values $\{C_{2p}\}$ and E_b may be found in exactly the same way as was done in the first method: one of the coefficients C_{2p} is put to unity, other C_{2p} are found from the linear system (59) with $k=1,2,\ldots,l$, and the resulting nonlinear equation is solved for E_b. The obtained values of E_b, which we designate as $(\hat{E}_b^S)_{l,R}$, and reduced functions $\hat{\psi}_{l,R}$ tend to their limits as the cutoff index l increases:

$$\lim_{l\to\infty}(\hat{E}_b^S)_{l,R}=(E_b^S)_R, \tag{60}$$

$$\lim_{l\to\infty}\hat{\psi}_{l,R}(r,t)=\Phi_R(r,t). \tag{61}$$

Values $(E_b^S)_R$ and $\Phi_R(r,t)$ in the right-hand sides of Eqs. (60) and (61) are equal to the corresponding limits in the right-hand sides of (47) and (48). The exact solution is given by formulas (49) and (50).

One of the advantages of this scheme over the first method is that it entails a considerably smaller amount of arithmetical calculations. Another merit resides in a substantially faster convergence of limits (60) and (61) than that of Eqs. (47) and (48).

However, even the second method can be substantially improved, and before proceeding to the discussion of convergence in Sec. VI we shall consider a factorization of the wave function, which partially accounts for the asymptotic behavior of ψ and significantly accelerates convergence of the solution.

C. Factorization of the wave function

Let us return to Eq. (29), which describes asymptotic links between radial functions $g_{2k}(r)$. Taking the asymptotic law (31) and the value of κ given by (32), we reduce Eq. (29) to the following form:

$$B_{2k+2}=\frac{B_{2k-2}/4-(1+|m|)B_{2k}}{4(k+1)(k+|m|+1)}. \tag{62}$$

As can be seen from (62), $B_2=-B_0/4$, $B_4=B_0/(4^2\times 2)$, and, generally,

$$B_{2k}=\frac{(-1)^k}{4^k k!}B_0 \tag{63}$$

(this formula is easily proved by induction on k).

At the first glance it seems possible to substitute Eqs. (31) and (63) into the series (25) and obtain the asymptotic behavior of ψ at large values of r:

$$\psi(r,\theta)\sim B_0 r^{\eta}\exp(-\kappa r)\sum_{k=0}^{\infty}\frac{1}{k!}\left(-\frac{1}{4}\gamma r^2\sin^2\theta\right)^k$$

$$=B_0 r^{\eta}\exp(-\kappa r)\exp\left(-\frac{1}{4}\gamma r^2\sin^2\theta\right). \tag{64}$$

However, this result is wrong because the asymptotic formula (29) was derived on the assumption that k is fixed and r goes to infinity, while Eq. (64) requires k to go to infinity at a fixed r. The inaccuracy of Eq. (64) can be easily verified by substituting it into the Schrödinger equation (6).

Nevertheless, we assume that Eq. (64) represents an approximate asymptote of ψ. This asymptote may be accounted for by introducing a new function $\chi(r,\theta)$ according to

$$\psi(r,\theta)=\exp(-\tfrac{1}{4}\gamma r^2\sin^2\theta)\chi(r,\theta). \tag{65}$$

Substituting this expression into the Schrödinger equation (6), we obtain the following equation for $\chi(r,\theta)$:

$$\chi_{rr}+\left(2\frac{|m|+\nu+1}{r}-\gamma r\sin^2\theta\right)\chi_r+\frac{1}{r^2}\chi_{\theta\theta}$$
$$+\left[\frac{(2|m|+1)\cot\theta-2\nu\tan\theta}{r^2}-\gamma\sin\theta\cos\theta\right]\chi_\theta$$
$$=\left(-\frac{2}{r}+2E_b\right)\chi. \tag{66}$$

We use the technique employed in Sec. III and look for χ in the form of a power series in r with coefficients, which depend on $t=\sin\theta$,

$$\chi(r,\theta)=\sum_{i=0}^{\infty}f_i(t)r^i. \tag{67}$$

Substituting Eq. (67) into the Schrödinger equation (66) and equating coefficients of equal powers of r, we obtain a nonhomogeneous differential equation for $f_i(t)$, which differs from Eq. (8) only in the right-hand side:

$$(1-t^2)f_i''+\left[\frac{2|m|+1}{t}-2(|m|+\nu+1)t\right]f_i'$$
$$+i[i+2(|m|+\nu)+1]f_i$$
$$=\gamma(t-t^3)f_{i-2}'+[2E_b+\gamma(i-2)t^2]f_{i-2}-2f_{i-1}. \tag{68}$$

The analysis carried out in Sec. III is applicable to the present situation as well. The function $f_i(t)$ is the sum of a particular integral and a complementary function. Boundary condition $(d\chi/dt)(0)=0$ implies that $f_i(t)$ includes only the even powers of t. A complementary function $F_i(t)$ is the product of a constant C_i by the polynomial $H_i(t)$ given by Eqs. (23) and (24), and f_i is given by Eq. (13).

The only difference between the present case and the one discussed in Sec. III is that the recurrent relation (15) for the coefficients $a_{i,j}$ is replaced with the following equation:

$$(i-j)[i+j+2(|m|+\nu)+1]a_{i,j}+(j+2)(j+2|m|+2)a_{i,j+2}$$
$$=\gamma(i-j)(a_{i-2,j-2}+C_{i-2}b_{i-2,j-2})$$
$$+(2E_b+\gamma j)(a_{i-2,j}+C_{i-2}b_{i-2,j})$$
$$-2(a_{i-1,j}+C_{i-1}b_{i-1,j}). \tag{69}$$

The function χ is given by the power series in two variables,

$$\chi(r,\theta)=\sum_{k=0}^{\infty}\sin^{2k}\theta\sum_{i=2k}^{\infty}\widetilde{A}_{i,2k}r^i, \tag{70}$$

$$\widetilde{A}_{i,2k}=\begin{cases} a_{i,2k}+C_i h_{i,2k}, & i=2p \\ a_{i,2k}, & i=2p+1, \end{cases} \tag{71}$$

where values of $a_{i,j}$ are determined from (69).

In order to transform the one-dimensional boundary condition at infinity $\chi(\infty,\theta)=0$ into an infinite set of zero-dimensional conditions we rewrite χ in the form, similar to Eq. (25),

$$\chi(r,\theta)=\sum_{k=0}^{\infty}\gamma^k(r\sin\theta)^{2k}y_{2k}(r). \tag{72}$$

Substituting this expression into (66), we obtain the following equation for $y_{2l}(r)$:

$$\frac{1}{2\gamma}y''_{2k}+\frac{2k+|m|+\nu+1}{\gamma r}y'_{2k}+\left(\frac{1}{\gamma r}-\frac{E_b}{\gamma}-k\right)y_{2k} =\frac{1}{2\gamma r}y'_{2k-2}-2(k+1)(k+|m|+1)y_{2k+2}. \tag{73}$$

The function $y_0(r)$ coincides with $g_0(r)$, whose asymptotic behavior is given by Eqs. (31) and (32), and for $k=0$ and $r\to\infty$ Eq. (73) yields

$$y_2\sim B_2 r^{\eta-1}\exp(-\kappa r), \tag{74}$$

$$B_2=B_0\frac{(\eta+|m|+\nu+1)\kappa-1}{2\gamma(|m|+1)}.$$

The asymptotic behavior of y_{2k} for $k>1$ is given by

$$y_{2k}\sim B_{2k}r^{\eta-1}\exp(-\kappa r),\quad B_{2k}=\frac{(k-1)B_{2k-2}}{2k(k+|m|)}. \tag{75}$$

Therefore, the exponential law, which determines the asymptotic behavior of functions g_{2l}, remains valid for y_{2k}, and boundary conditions for y_{2k} coincide with the conditions (33) for g_{2k}:

$$\lim_{r\to\infty}\frac{y'_{2k}(r)}{y_{2k}(r)}=-\kappa. \tag{76}$$

Now the problem is formulated in exactly the same manner as was done for the function $\psi(r,\theta)$, and the algebraic algorithms described in Secs. V A and V B are applicable to the present situation without any modification.

It turned out that the factorization of the wave function described above dramatically accelerates the convergence of solution when the cutoff index l increases. The fastest convergence is achieved by the combination of the factorization and the algorithm described in Sec. VB.

VI. CONVERGENCE AND NUMERICAL TECHNIQUE

The algebraic algorithms described in Secs. VA and VB are based on three reductions of infinite quantities to finite values which can be practically dealt with. The first reduction is the termination of infinite sums in Eqs. (40) and (57) at a finite index i. The second truncation occurs when we consider reduced functions $\widetilde{\psi}_{l,R}$ and $\hat{\psi}_{l,R}$ [Eqs. (43) and (58)] and take a finite number l of unknown coefficients and functions. Finally, the third reduction is the replacement of boundary conditions at infinity with boundary conditions imposed at a finite radius (34). In this section we address these aspects of the algorithms and discuss the question of convergence of the solution.

A. Calculation of ''traces''

In calculating radial functions $q^n_{2k}(R)$ and $w_{l,2k}(R)$ we need to terminate the summation over i in Eqs. (40) and (57) at a finite value of i. In order to control the error introduced by this operation it is important to know the upper bound on the remainder of the series. It follows from Eqs. (15) and (69) that the asymptotic rate of convergence is exponentially fast because for large values of i the multiplier before $a_{i,j}$ in the left-hand sides of (15) and (69) is proportional to i^2 while the right-hand side of (15) does not contain i at all and the right-hand side of (69) involves i only linearly. This qualitative consideration can be rigorously proven.

Here we present the analysis of convergence of the infinite sum in Eq. (55) with coefficients given by (69) (the second method with factorization). Let us denote the $l+1$ coefficients $(\mathsf{T}^n_l)_{i,j}$, $j=0,2,\ldots,2l$ as a vector $\mathfrak{T}_i$; its kth component is $(\mathsf{T}^n_l)_{i,2k}$. The recurrent relation (69) can be presented in the form

$$\mathbf{J}_i\mathfrak{T}_i=\gamma\mathbf{E}_i\mathfrak{T}_{i-2}-2\,\mathfrak{T}_{i-1}, \tag{77}$$

where $\mathbf{J}_i$ and $\mathbf{E}_i$ are matrices $(l+1)\times(l+1)$ with the following nonzero elements:

$$\begin{aligned} (\mathbf{J}_i)_{p,p} &= (i-2p)[i+2p+2(|m|+\nu)+1], \\ (\mathbf{J}_i)_{p,p+1} &= 4(p+2)(p+|m|+2), \\ (\mathbf{E}_i)_{p,p} &= i-2p, \\ (\mathbf{E}_i)_{p,p-1} &= \frac{2E_b}{\gamma}+2p. \end{aligned} \tag{78}$$

Equation (77) may be rewritten in the form

$$\mathfrak{T}_i=\gamma\mathbf{J}_i^{-1}\mathbf{E}_i\mathfrak{T}_{i-2}-2\mathbf{J}_i^{-1}\mathfrak{T}_{i-1}. \tag{79}$$

Lemma 1. Let $\|\mathfrak{B}\|\triangleq\max_{0\leqslant i\leqslant l+1}|\mathfrak{B}_i|$ be the norm of a vector $\mathfrak{B}$ of length $l+1$. Then for $i>3(l+|m|+1)$

$$\|\mathbf{J}_i^{-1}\mathfrak{B}\|<\frac{1}{i^2-4l^2-4(l+|m|+1)^2}\|\mathfrak{B}\|\triangleq K_i\|\mathfrak{B}\|.$$

Proof. The nonzero elements of the inverse matrix $\mathbf{J}_i^{-1}$ are given by the following formula:

$$(\mathbf{J}_i^{-1})_{p,q}=(-1)^{q-p}\frac{\Pi_{n=p}^{q-1}(\mathbf{J}_i)_{n,n+1}}{\Pi_{n=p}^{q}(\mathbf{J}_i)_{n,n}},\quad q\geqslant p. \tag{80}$$

The following estimation is valid ($u=l+|m|+1$):

$$|(\mathbf{J}_i^{-1})_{p,q}| = \frac{\Pi_{n=p}^{q-1}(\mathbf{J}_i)_{n,n+1}}{\Pi_{n=p}^{q}(\mathbf{J}_i)_{n,n}} \leqslant \frac{[\max_{p\leqslant n\leqslant q-1}(\mathbf{J}_i)_{n,n+1}]^{q-p}}{[\min_{p\leqslant n\leqslant q}(\mathbf{J}_i)_{n,n}]^{q-p+1}}$$

$$\leqslant \frac{[4(q+1)(q+|m|+1)]^{q-p}}{\{(i-2q)[i+2q+2(|m|+\nu)+1]\}^{q-p+1}}$$

$$< \frac{[2(q+|m|+1)]^{2(q-p)}}{(i^2-4q^2)^{q-p+1}} \leqslant \frac{(2u)^{2(q-p)}}{(i^2-4l^2)^{q-p+1}}$$

$$= \frac{1}{i^2-4l^2}\left(\frac{4u^2}{i^2-4l^2}\right)^{q-p} \triangleq \overline{(J_i^{-1})}_{p.q}. \tag{81}$$

Further,

$$\|\mathbf{J}_i^{-1}\mathfrak{B}\| \leqslant \|\mathbf{J}_i^{-1}\boldsymbol{j}\|\,\|\mathfrak{B}\|,$$

$$\|\mathbf{J}_i^{-1}\boldsymbol{j}\| \leqslant \max_{0\leqslant p\leqslant l}\sum_{q=0}^{l}|(\mathbf{J}_i^{-1})_{p,q}|$$

$$< \max_{0\leqslant p\leqslant l}\sum_{s=0}^{l-p}(\mathbf{J}_i^{-1})_{p,p+s}$$

$$< \frac{1}{i^2-4l^2}\sum_{s=0}^{\infty}\left(\frac{4u^2}{i^2-4l^2}\right)^s = \frac{1}{i^2-4(l^2+u^2)}.$$

□

Lemma 2. If

$$i > 4(l+|m|+1) + \frac{1}{\gamma}\left(\frac{2}{r}+2E_b+1\right) + \sqrt{2r}, \tag{82}$$

then the following inequality is valid:

$$\|\mathfrak{T}_i + r\mathfrak{T}_{i+1}\| < \frac{4\gamma}{i}\|\mathfrak{T}_{i-2} + r\mathfrak{T}_{i-1}\|. \tag{83}$$

Proof. As follows from (79),

$$\|\mathfrak{T}_i\| \leqslant \gamma K_i\|\mathbf{E}_i\mathfrak{T}_{i-2}\| + 2K_i\|\mathfrak{T}_{i-1}\|.$$

For any vector $\mathfrak{B}$

$$\|\mathbf{E}_i\mathfrak{B}\| \leqslant \|\mathfrak{B}\|\max_{0\leqslant p\leqslant l}\sum_{q=0}^{l}(\mathbf{E}_i)_{p,q}$$

$$= \left(i + \frac{2E_b}{\gamma}\right)\|\mathfrak{B}\| \triangleq L_i\|\mathfrak{B}\|.$$

Straightforward algebra gives

$$\|\mathfrak{T}_i + r\mathfrak{T}_{i+1}\| \leqslant W_1\|\mathfrak{T}_{i-2}\| + W_2 r\|\mathfrak{T}_{i-1}\|,$$

where

$$W_1 = \gamma K_i L_i(1 + 2rK_{i+1}),$$

$$W_2 = \frac{2K_i}{r} + K_{i+1}(\gamma L_{i+1} + 4K_i).$$

If we again denote $u = l + |m| + 1$, then

$$W_1 < \frac{\gamma}{i}\,\frac{1+2E_b/\gamma i}{1-8u^2/i^2}\left(1 + \frac{2r}{i^2-8u^2}\right) < \frac{4\gamma}{i},$$

$$W_2 < \frac{\gamma}{i}\,\frac{1}{1-8u^2/i^2}\left(1 + 2\frac{1/r+E_b}{i\gamma} + \frac{1}{i^3\gamma}\,\frac{4}{1-8u^2/i^2}\right)$$

$$< \frac{2\gamma}{i}\left(1 + 2\frac{1/r+E_b}{i\gamma} + \frac{8}{i^3\gamma}\right) < \frac{4\gamma}{i}.$$

Therefore,

$$\|\mathfrak{T}_i + r\mathfrak{T}_{i+1}\| \leqslant (\|\mathfrak{T}_{i-2}\| + r\|\mathfrak{T}_{i-1}\|)\max(W_1, W_2)$$

$$< \frac{4\gamma}{i}\|\mathfrak{T}_{i-2} + r\mathfrak{T}_{i-1}\|.$$

□

Lemma 3. If (82) is satisfied and $i > 8\gamma r^2$, then

$$\max_{0\leqslant k\leqslant l}\sum_{s=i}^{\infty}(\mathsf{T}_l^n)_{s,2k}r^s < r^2\max_{0\leqslant k\leqslant l}\sum_{s=i-2}^{i-1}(\mathsf{T}_l^n)_{s,2k}r^s. \tag{84}$$

Proof. With the aid of Lemma 2 we obtain

$$\max_{0\leqslant k\leqslant l}\sum_{s=i}^{\infty}(\mathsf{T}_l^n)_{s,2k}r^s = \|\sum_{s=i}^{\infty}\mathfrak{T}_s r^s\|$$

$$\leqslant r^i\sum_{p=0}^{\infty}\|\mathfrak{T}_{i+2p} + r\mathfrak{T}_{i+2p+1}\|r^{2p}$$

$$< r^i\|\mathfrak{T}_{i-2} + r\mathfrak{T}_{i-1}\|\sum_{p=0}^{\infty}\prod_{q=0}^{p}\frac{4\gamma r^2}{i+2q}$$

$$< r^i\|\mathfrak{T}_{i-2} + r\mathfrak{T}_{i-1}\|$$

$$= r^2\max_{0\leqslant k\leqslant l}\sum_{s=i-2}^{i-1}(\mathsf{T}_l^n)_{s,2k}r^s.$$

□

Lemma 3 gives an upper bound on the remainder of the series in Eq. (55). Analogous formulas can be easily obtained for the second algorithm without factorization and for the first algorithm.

To get more insight into the asymptotic behavior of series we present typical results obtained numerically. Figure 1(a) shows the dependence of terms $(\mathsf{T}_l^n)_{i,j}$ [given by (54)], addends $(\mathsf{T}_l^n)_{i,j}R^i$, and partial sums $\Sigma_{k=0}^{i}(\mathsf{T}_l^n)_{k,j}R^i$ on the index i for the following set of values: $\gamma = 1$, $R = 10$, $l = 10$, and $j = n = |m| = \nu = 0$. The computation was performed according to the second algorithm without factorization.

The behavior exhibited by terms of the series is very typical for both algorithms and demonstrates the already proven fact that for large values of i the magnitude of addends decreases exponentially fast. In particular, it shows that the estimate given by Lemma 3 is very crude and the condition (84) is satisfied already for $i \leqslant 8\gamma r^2$. This is caused by very rough estimates made in Lemma 2, where terms like $(1+2E_b/\gamma i)/(1\text{-}8u^2/i^2)$ were majorized by 2. In practice, the calculation may be terminated if several last addends have not altered the sum within the computational precision.

The numerical data shown in Fig. 1(a) are presented in

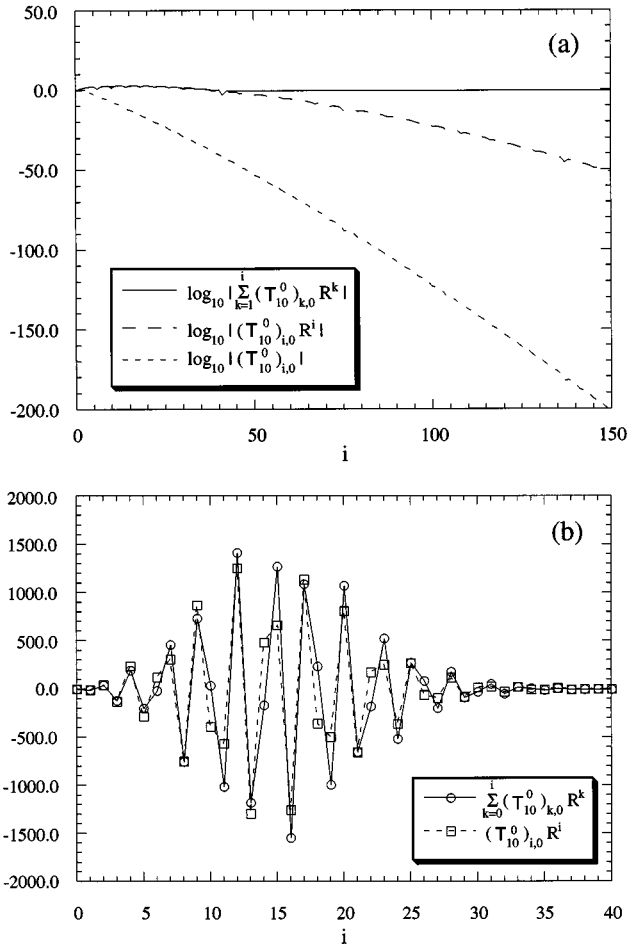

FIG. 1. The behavior of terms $(T^0_{10})_{i,0}$ and partial sums $\Sigma^i_{k=0}(T^0_{10})_{k,0}R^k$ for $\gamma=1$, $R=10$, and $m=\nu=0$ (dimensionless units): (a) on a logarithmic scale, (b) on a linear scale.

Fig. 1(b) on a linear scale. The picture demonstrates that although some intermediate addends are very large in magnitude, they nevertheless perfectly cancel themselves, and the final result $\Sigma^\infty_{i=0}(T^0_{10})_{i,0}R^i \approx -0.5664$ is less by almost

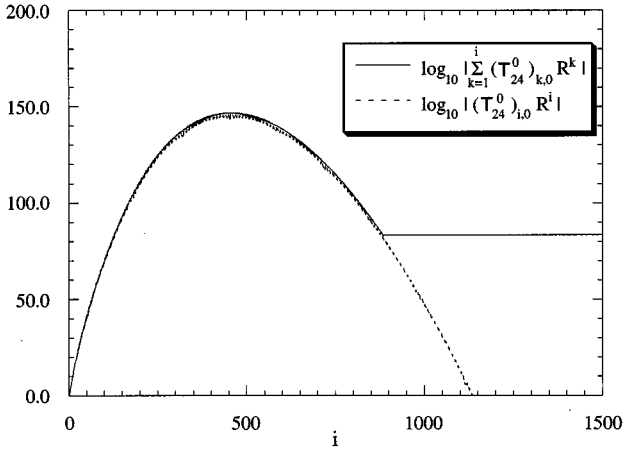

FIG. 2. Behavior of terms $(T^0_{24})_{i,0}R^i$ and partial sums $\Sigma^i_{k=0}(T^0_{10})_{k,0}R^k$ for $\gamma=100$, $R=8$, and $m=\nu=0$ (dimensionless units).

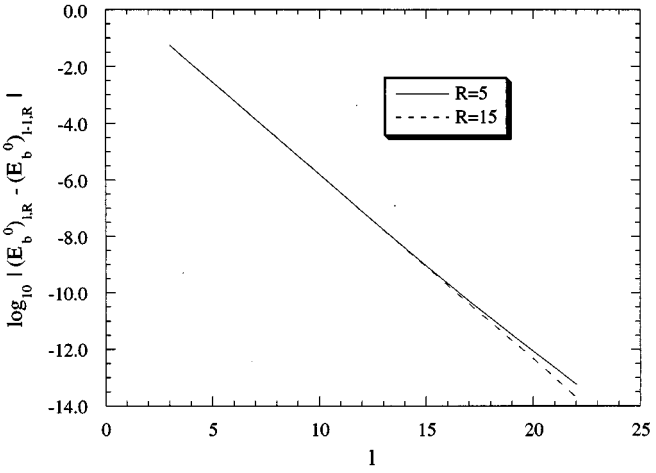

FIG. 3. The dependence of the difference between successive values $(\hat{E}^0_b)_{l,R}$ and $(\hat{E}^0_b)_{l-1,R}$ on the cutoff index l for $\gamma=1$, $m=\nu=0$, $R=5$, and $R=15$.

four orders of magnitude than some intermediate partial sums $\Sigma^i_{k=0}(T^0_{10})_{k,0}R^k$.

In Fig. 2 the same effect is shown for the case $\gamma=100$, $R=8$, $l=24$, $j=n=|m|=\nu=0$. Although the intermediate terms reach 10^{147}, the final result is -5.158×10^{83}, i.e., by 64 orders of magnitude less. (The computation was performed with precision $\approx$300 decimal digits.) Due to the complicated form of matrices $\mathbf{J}_i$ and $\mathbf{J}_i^{-1}$ concise presentation of the sum explaining the cancellation of terms is not obtained yet.

B. Convergence of solution

The principal question is the convergence of solutions with increasing cutoff index l and radius R. Since a rigorous investigation of convergence is not yet completed, the discussion is based on the analysis of obtained numerical data.

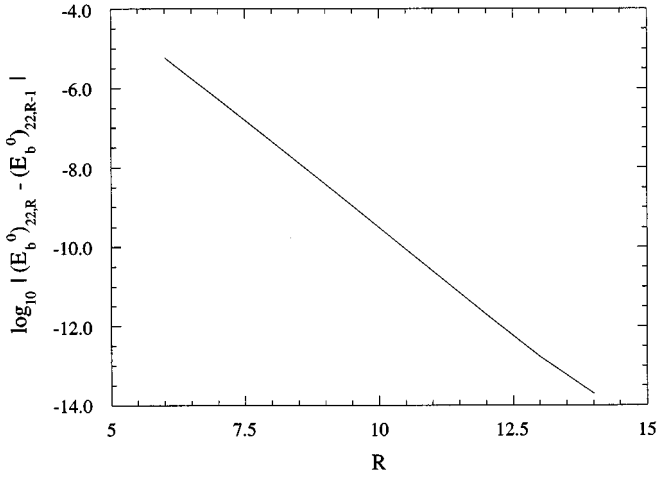

FIG. 4. The dependence of the difference between values $(\hat{E}^0_b)_{l,R}$ and $(\hat{E}^0_b)_{l,R-1}$ on the joining radius R for $\gamma=1$, $l=22$, $m=\nu=0$.

TABLE I. Binding energies (atomic units) of the ground state $1s_0$. The maximal absolute error of each value is $\pm 10^{-12}$ (± 1 in the last digit).

γ	$1s_0$	γ	$1s_0$
1.0×10^{-4}	0.500 049 997 500	1.0	0.831 168 896 733
1.25×10^{-4}	0.500 062 496 094	1.25	0.885 966 911 455
1.5×10^{-4}	0.500 074 994 375	1.5	0.935 357 250 593
2.0×10^{-4}	0.500 099 990 000	2.0	1.022 213 907 665
2.5×10^{-4}	0.500 124 984 375	2.5	1.097 537 010 632
3.0×10^{-4}	0.500 149 977 499	3.0	1.164 532 989 349
4.0×10^{-4}	0.500 199 960 000	4.0	1.280 798 016 052
5.0×10^{-4}	0.500 249 937 500	5.0	1.380 398 866 427
6.0×10^{-4}	0.500 299 910 000	6.0	1.468 245 988 856
8.0×10^{-4}	0.500 399 840 000	8.0	1.619 384 995 667
1.0×10^{-3}	0.500 499 750 000	10.0	1.747 797 163 714
1.25×10^{-3}	0.500 624 609 376	12.5	1.886 577 311 278
1.5×10^{-3}	0.500 749 437 501	15.0	2.008 064 107 786
2.0×10^{-3}	0.500 999 000 004	20.0	2.215 398 515 433
2.5×10^{-3}	0.501 248 437 511	25.0	2.390 136 630 706
3.0×10^{-3}	0.501 497 750 022	30.0	2.542 421 668 319
4.0×10^{-3}	0.501 996 000 071	40.0	2.801 029 824 778
5.0×10^{-3}	0.502 493 750 172	50.0	3.017 860 707 047
6.0×10^{-3}	0.502 991 000 357	60.0	3.206 081 694 334
8.0×10^{-3}	0.503 984 001 130	80.0	3.524 277 153 307
0.01	0.504 975 002 759	100.0	3.789 804 236 305
0.0125	0.506 210 944 235	125.0	4.072 468 138 441
0.015	0.507 443 763 961	150.0	4.316 646 712 620
0.02	0.509 900 044 089	200.0	4.727 145 110 687
0.025	0.512 343 857 534	250.0	5.067 673 826 226
0.03	0.514 775 222 717	300.0	5.360 814 684 149
0.04	0.519 600 701 769	400.0	5.851 651 162 832
0.05	0.524 376 706 706	500.0	6.257 087 674 681
0.06	0.529 103 522 564	600.0	6.604 936 099 852
0.08	0.538 411 004 390	800.0	7.185 134 522 785
0.1	0.547 526 480 401	1000.0	7.662 423 247 755
0.125	0.558 657 016 093	2000.0	9.304 765 082 770
0.15	0.569 502 945 779	4000.0	11.204 145 206 603
0.2	0.590 381 565 035		
0.25	0.610 247 435 260		
0.3	0.629 186 552 901		
0.4	0.664 605 379 868		
0.5	0.697 210 538 458		
0.6	0.727 462 287 757		
0.8	0.782 283 393 769		

TABLE II. Binding energies of the state $2s_0$. The uncertainty of each value is ± 1 in the last digit.

γ	$2s_0$	γ	$2s_0$
1.0×10^{-4}	0.125 049 965 000	1.0	0.160 468 982 634
1.25×10^{-4}	0.125 062 445 312	1.25	0.164 543 710 079
1.5×10^{-4}	0.125 074 921 250	1.5	0.168 083 038 952
2.0×10^{-4}	0.125 099 860 000	2.0	0.173 944 705 973
2.5×10^{-4}	0.125 124 781 251	2.5	0.178 655 849 584
3.0×10^{-4}	0.125 149 685 001	3.0	0.182 576 926 410
4.0×10^{-4}	0.125 199 440 004	4.0	0.188 846 463 700
5.0×10^{-4}	0.125 249 125 010	5.0	0.193 746 709 717
6.0×10^{-4}	0.125 298 740 021	6.0	0.197 757 831 051
8.0×10^{-4}	0.125 397 760 065	8.0	0.204 076 207 347
1.0×10^{-3}	0.125 496 500 159	10.0	0.208 951 829 045
1.25×10^{-3}	0.125 619 531 639	12.5	0.213 793 293 8
1.5×10^{-3}	0.125 742 125 806	15.0	0.217 717 571 0
2.0×10^{-3}	0.125 986 002 548	20.0	0.223 842 126 8
2.5×10^{-3}	0.126 228 131 218	25.0	0.228 529 129 8
3.0×10^{-3}	0.126 468 512 890	30.0	0.232 313 979 6
4.0×10^{-3}	0.126 944 040 697	40.0	0.238 199 272 8
5.0×10^{-3}	0.127 412 599 234	50.0	0.242 687 793 8
6.0×10^{-3}	0.127 874 205 455	60.0	0.246 303 868 2
8.0×10^{-3}	0.128 776 646 819	80.0	0.251 913 320 1
0.01	0.129 651 571 358	100.0	0.256 181 570 3
0.0125	0.130 706 932 235	125.0	0.260 376 3
0.015	0.131 720 323 013	150.0	0.263 748 6
0.02	0.133 624 177 535	200.0	0.268 968 2
0.025	0.135 369 943 751	250.0	0.272 930 7
0.03	0.136 965 459 672	300.0	0.276 112 2
0.04	0.139 739 824 579	400.0	0.281 029 7
0.05	0.142 016 720 515	500.0	0.284 757 5
0.06	0.143 863 462 506	600.0	0.287 747 4
0.08	0.146 507 410 460	800.0	0.292 363
0.1	0.148 089 155 790	1000.0	0.295 857
0.125	0.149 057 200 581		
0.15	0.149 331 214 566		
0.2	0.148 986 678 198		
0.25	0.148 506 569 448		
0.3	0.148 367 306 786		
0.4	0.149 166 347 848		
0.5	0.150 807 855 777		
0.6	0.152 765 570 424		
0.8	0.156 770 811 245		

The first question we address is the convergence of solution as the cutoff index l increases. Figure 3 shows the logarithm of difference between successive values $(\hat{E}_b^0)_{l,R}$ and $(\hat{E}_b^0)_{l-1,R}$ for $\gamma=1$, $m=\nu=0$, calculated according to the second method with factorization. As can be seen, this difference decreases exponentially with increasing l, and the rate of decrease grows slightly as R becomes larger. This fact allows us to obtain the upper bound on the truncation error:

$$|(\hat{E}_b^S)_{\infty,R}-(\hat{E}_b^S)_{l,R}|\leq\alpha|(\hat{E}_b^S)_{l,R}-(\hat{E}_b^S)_{l-1,R}|. \qquad (85)$$

The value of α depends on the quantum state and can be obtained from computation (for the ground state $\alpha\approx0.3$, for low-lying states $\alpha\lesssim1$).

Figure 4 demonstrates the dependence of $(\hat{E}_b^0)_{l,R}$ on the joining radius R for the case $\gamma=1$, $m=\nu=0$, $l=22$. The value of $\log_{10}|(\hat{E}_b^0)_{l,R}-(\hat{E}_b^0)_{l,R-1}|$ is plotted against R and shows that this difference decreases exponentially as R in-

TABLE III. Binding energies of the state $2p_0$. The uncertainty of each value is ± 1 in the last digit.

γ	$2p_0$	γ	$2p_0$
1.0×10^{-4}	0.125 049 985 000	1.0	0.260 006 615 944
1.25×10^{-4}	0.125 062 476 563	1.25	0.271 978 002 965
1.5×10^{-4}	0.125 074 966 250	1.5	0.281 900 248 134
2.0×10^{-4}	0.125 099 940 000	2.0	0.297 710 972 385
2.5×10^{-4}	0.125 124 906 250	2.5	0.310 016 491 599
3.0×10^{-4}	0.125 149 865 000	3.0	0.320 040 180 152
4.0×10^{-4}	0.125 199 760 001	4.0	0.335 695 728 671
5.0×10^{-4}	0.125 249 625 003	5.0	0.347 617 775 313
6.0×10^{-4}	0.125 299 460 005	6.0	0.357 161 821 897
8.0×10^{-4}	0.125 399 040 017	8.0	0.371 769 785 534
1.0×10^{-3}	0.125 498 500 042	10.0	0.382 649 848 306
1.25×10^{-3}	0.125 622 656 353	12.5	0.393 078 49
1.5×10^{-3}	0.125 746 625 213	15.0	0.401 232 88
2.0×10^{-3}	0.125 994 000 672	20.0	0.413 377 73
2.5×10^{-3}	0.126 240 626 640	25.0	0.422 156 44
3.0×10^{-3}	0.126 486 503 399	30.0	0.428 898 19
4.0×10^{-3}	0.126 976 010 735	40.0	0.438 733 80
5.0×10^{-3}	0.127 462 526 184	50.0	0.445 685 11
6.0×10^{-3}	0.127 946 054 235	60.0	0.450 929 99
8.0×10^{-3}	0.128 904 170 933	80.0	0.458 430 21
0.01	0.129 850 415 833	100.0	0.463 617 76
0.0125	0.131 016 634 643	125.0	0.468 282 5
0.015	0.132 164 579 759	150.0	0.471 726 0
0.02	0.134 406 465 981	200.0	0.476 532 0
0.025	0.136 577 969 688	250.0	0.479 771 0
0.03	0.138 681 330 848	300.0	0.482 127 2
0.04	0.142 693 709 740	400.0	0.485 363 0
0.05	0.146 464 837 782	500.0	0.487 507 1
0.06	0.150 016 268 441	600.0	0.489 047 0
0.08	0.156 540 574 354	800.0	0.491 132 8
0.1	0.162 410 078 399	1000.0	0.492 495 0
0.125	0.168 998 302 963		
0.15	0.174 911 277 818		
0.2	0.185 184 041 068		
0.25	0.193 911 175 542		
0.3	0.201 504 145 350		
0.4	0.214 265 501 994		
0.5	0.224 760 340 776		
0.6	0.233 678 467 049		
0.8	0.248 291 923 804		

TABLE IV. Binding energies of the state $2p_{-1}$. The uncertainty of each value is ± 1 in the last digit.

γ	$2p_{-1}$	γ	$2p_{-1}$
1.0×10^{-4}	0.125 099 970 000	1.0	0.456 597 058 424
1.25×10^{-4}	0.125 124 953 125	1.25	0.498 311 263 507
1.5×10^{-4}	0.125 149 932 500	1.5	0.535 345 522 071
2.0×10^{-4}	0.125 199 880 000	2.0	0.599 612 773 602
2.5×10^{-4}	0.125 249 812 500	2.5	0.654 769 276 594
3.0×10^{-4}	0.125 299 730 001	3.0	0.703 546 577 517
4.0×10^{-4}	0.125 399 520 003	4.0	0.787 825 272 030
5.0×10^{-4}	0.125 499 250 007	5.0	0.859 832 622 577
6.0×10^{-4}	0.125 598 920 015	6.0	0.923 291 780 185
8.0×10^{-4}	0.125 798 080 048	8.0	1.032 503 930 764
1.0×10^{-3}	0.125 997 000 116	10.0	1.125 422 341 840
1.25×10^{-3}	0.126 245 312 783	12.5	1.226 045 644 052
1.5×10^{-3}	0.126 493 250 587	15.0	1.314 336 111 787
2.0×10^{-3}	0.126 988 001 855	20.0	1.465 508 545 545
2.5×10^{-3}	0.127 481 254 527	25.0	1.593 422 436 295
3.0×10^{-3}	0.127 973 009 384	30.0	1.705 287 570 967
4.0×10^{-3}	0.128 952 029 630	40.0	1.896 082 532 426
5.0×10^{-3}	0.129 925 072 248	50.0	2.056 846 667 495
6.0×10^{-3}	0.130 892 149 587	60.0	2.196 970 312 115
8.0×10^{-3}	0.132 808 470 954	80.0	2.435 025 269 312
0.01	0.134 701 144 177	100.0	2.634 760 665 299
0.0125	0.137 034 022 428	125.0	2.848 423 318 040
0.015	0.139 330 697 178	150.0	3.033 821 231 621
0.02	0.143 817 610 347	200.0	3.347 145 23
0.025	0.148 166 846 117	250.0	3.608 550 84
0.03	0.152 384 114 685	300.0	3.834 605 66
0.04	0.160 447 535 409	400.0	4.215 128 28
0.05	0.168 058 188 454	500.0	4.531 246 38
0.06	0.175 264 418 760	600.0	4.803 692 91
0.08	0.188 633 896 259	800.0	5.260 512 40
0.1	0.200 845 672 373	1000.0	5.638 421 08
0.125	0.214 808 439 701		
0.15	0.227 607 738 247		
0.2	0.250 539 101 715		
0.25	0.270 805 013 466		
0.3	0.289 092 475 828		
0.4	0.321 354 781 180		
0.5	0.349 477 297 763		
0.6	0.374 623 772 834		
0.8	0.418 588 648 705		

creases. The rate of decrease depends on the quantum state; as a necessary condition, R must be greater than the position of the farthest extremum of the wave function. The almost perfect exponential behavior exhibited by the curve in Fig. 4 is typical for all energy levels and allows one to obtain a reliable upper bound on the difference $|(\hat{E}_b^S)_{l,\infty}-(\hat{E}_b^S)_{l,R}|$.

C. Numerical technique

As was mentioned in Sec. VI A, terms of the infinite sums almost perfectly cancel themselves. There is little doubt that there exist concise analytical formulas for summation, and we have serious reasons to believe that the ongoing theoretical investigation will allow us to obtain these formulas. Results reported in the present work were obtained by direct summation of series.

Although the algorithm of solution described in Sec. V is rather simple and straightforward and the summation of series is basically a very simple procedure, the problem does require a nontrivial numerical treatment. The need to keep track of a large number of canceling digits leads to the re-

TABLE V. Binding energies of the state $3p_0$. The uncertainty of each value is ± 1 in the last digit.

γ	$3p_0$	γ	$3p_0$
1.0×10^{-4}	0.055 605 465 6	0.1	0.069 891 690 4
1.25×10^{-4}	0.055 617 914 9	0.125	0.071 332 184 9
1.5×10^{-4}	0.055 630 353 0	0.15	0.072 640 918 4
2.0×10^{-4}	0.055 655 195 6	0.2	0.074 925 455 4
2.5×10^{-4}	0.055 679 993 1	0.25	0.076 852 801 7
3.0×10^{-4}	0.055 704 745 6	0.3	0.078 506 708 7
4.0×10^{-4}	0.055 754 115 6	0.4	0.081 222 856 5
5.0×10^{-4}	0.055 803 305 8	0.5	0.083 390 113 0
6.0×10^{-4}	0.055 852 316 0	0.6	0.085 183 211 7
8.0×10^{-4}	0.055 949 797 0	0.8	0.088 026 643 3
1.0×10^{-3}	0.056 046 559 1	1.0	0.090 224 511 3
1.25×10^{-3}	0.056 166 501 7	1.25	0.092 399 910 3
1.5×10^{-3}	0.056 285 323 4	1.5	0.094 151 932 5
2.0×10^{-3}	0.056 519 611 8	2.0	0.096 854 601 0
2.5×10^{-3}	0.056 749 442 6	2.5	0.098 887 587 8
3.0×10^{-3}	0.056 974 839 1	3.0	0.100 501 208 6
4.0×10^{-3}	0.057 412 445 7	4.0	0.102 950 666 0
5.0×10^{-3}	0.057 832 710 6	5.0	0.104 762 116 0
6.0×10^{-3}	0.058 235 979 3	6.0	0.106 180 992 0
8.0×10^{-3}	0.058 993 195 6	8.0	0.108 302 456 1
0.01	0.059 687 870 0	10.0	0.109 845 603 4
0.0125	0.060 474 826 0	12.5	0.111 297 12
0.015	0.061 179 679 5	15.0	0.112 414 34
0.02	0.062 378 561 9	20.0	0.114 051 11
0.025	0.063 350 742 4	25.0	0.115 215 16
0.03	0.064 151 833 7	30.0	0.116 098 89
0.04	0.065 406 380 0	40.0	0.117 373 14
0.05	0.066 380 498 4	50.0	0.118 263 57
0.06	0.067 203 259 8	60.0	0.118 930 16
0.08	0.068 625 377 9	80.0	0.119 876 00
		100.0	0.120 525 41

TABLE VI. Binding energies of the state $3p_{-1}$. The uncertainty of each value is ± 1 in the last digit.

γ	$3p_{-1}$	γ	$3p_{-1}$
1.0×10^{-4}	0.055 655 375 556	1.0	0.125 479 244 9
1.25×10^{-4}	0.055 680 274 307	1.25	0.130 880 617 2
1.5×10^{-4}	0.055 705 150 559	1.5	0.135 344 014 5
2.0×10^{-4}	0.055 754 835 567	2.0	0.142 452 180 5
2.5×10^{-4}	0.055 804 430 584	2.5	0.148 000 767 0
3.0×10^{-4}	0.055 853 935 614	3.0	0.152 545 169 6
4.0×10^{-4}	0.055 952 675 740	4.0	0.159 716 197 4
5.0×10^{-4}	0.056 051 056 004	5.0	0.165 264 273 1
6.0×10^{-4}	0.056 149 076 488	6.0	0.169 779 722 4
8.0×10^{-4}	0.056 344 038 502	8.0	0.176 858 853 0
1.0×10^{-3}	0.056 537 562 745	10.0	0.182 301 494 7
1.25×10^{-3}	0.056 777 448 097	12.5	0.187 694 09
1.5×10^{-3}	0.057 015 091 899	15.0	0.192 058 82
2.0×10^{-3}	0.057 483 670 174	20.0	0.198 863 10
2.5×10^{-3}	0.057 943 334 623	25.0	0.204 066 16
3.0×10^{-3}	0.058 394 132 313	30.0	0.208 266 21
4.0×10^{-3}	0.059 269 363 270	40.0	0.214 795 86
5.0×10^{-3}	0.060 109 922 884	50.0	0.219 775 73
6.0×10^{-3}	0.060 916 499 227	60.0	0.223 788 10
8.0×10^{-3}	0.062 430 977 317	80.0	0.230 013 78
0.01	0.063 820 114 240	100.0	0.234 752 62
0.0125	0.065 392 702 454	125.0	0.239 411 7
0.015	0.066 798 678 347	150.0	0.243 158 7
0.02	0.069 175 121 874	200.0	0.248 961 2
0.025	0.071 068 428 637		
0.03	0.072 579 377 065		
0.04	0.074 772 332 699		
0.05	0.076 257 724 143		
0.06	0.077 373 300 563		
0.08	0.079 258 016 467		
0.1	0.081 171 192 010		
0.125	0.083 684 869 7		
0.15	0.086 189 844 8		
0.2	0.090 841 835 7		
0.25	0.094 919 509 5		
0.3	0.098 491 031 2		
0.4	0.104 477 783 7		
0.5	0.109 361 674 0		
0.6	0.113 478 996 6		
0.8	0.120 164 833 7		

quirement for high computational precision. In order to suit this demand we had to develop a special high-precision floating-point arithmetic which is written as a portable code in C++ programming language and is specially optimized for the employed algorithm. The high-precision arithmetic introduces two kinds of numbers, medium-precision numbers, used to represent physical quantities (γ, R, E_b) in the internal format with moderate precision ($\approx$20 decimal digits), and high-precision numbers, which are used to store all intermediate values and can provide very high computational precision.

This technique allows very efficient calculation of sums in Eqs. (40) and (57). The time required to obtain seven significant digits of the ground-state binding energy for the field $\gamma=1$, i.e., for the most interesting region for the quadratic Zeeman effect where the magnetic and Coulomb interactions are comparable, takes about a second with a simple 386 IBM PC. For the field $\gamma=1000$ an analogous calculation takes the time of the order of a minute with a usual desktop workstation. The precision required to compute the ground-state binding energies with accuracy 10^{-12} hartree is $\approx$38 decimal digits for $\gamma=1$ and $\approx$280 decimal digits for $\gamma=100$; calculations of excited states $n\leqslant 10$ in the chaotic region $\gamma=0,\ldots,0.01$ require $40,\ldots,70$ decimal digits.

VII. RESULTS

In this section we present first results obtained with the aid of the exact solution. Due to the immense size of related data it is impossible to give the complete description of results here, so we present only exact tables of several low-

TABLE VII. Binding energies of the state $3d_{-1}$. The uncertainty of each value is ± 1 in the last digit.

γ	$3d_{-1}$	γ	$3md_{-1}$
1.0×10^{-4}	0.055 655 465 556	1.0	0.206 567 363 860
1.25×10^{-4}	0.055 680 414 931	1.25	0.218 706 110 0
1.5×10^{-4}	0.055 705 353 057	1.5	0.228 860 214 8
2.0×10^{-4}	0.055 755 195 559	2.0	0.245 240 759 5
2.5×10^{-4}	0.055 804 993 065	2.5	0.258 180 795 2
3.0×10^{-4}	0.055 854 745 575	3.0	0.268 857 916 7
4.0×10^{-4}	0.055 954 115 618	4.0	0.285 802 855 1
5.0×10^{-4}	0.056 053 305 709	5.0	0.298 946 574 0
6.0×10^{-4}	0.056 152 315 874	6.0	0.309 631 169 2
8.0×10^{-4}	0.056 349 796 563	8.0	0.326 289 158 6
1.0×10^{-3}	0.056 546 558 013	10.0	0.338 956 189 8
1.25×10^{-3}	0.056 791 499 053	12.5	0.351 325 68
1.5×10^{-3}	0.057 035 317 985	15.0	0.361 165 76
2.0×10^{-3}	0.057 519 594 775	20.0	0.376 119 81
2.5×10^{-3}	0.057 999 401 107	25.0	0.387 172 31
3.0×10^{-3}	0.058 474 753 188	30.0	0.395 812 10
4.0×10^{-3}	0.059 412 176 196	40.0	0.408 676 29
5.0×10^{-3}	0.060 332 058 593	50.0	0.417 972 13
6.0×10^{-3}	0.061 234 642 207	60.0	0.425 109 20
8.0×10^{-3}	0.062 989 081 640	80.0	0.435 517 97
0.01	0.064 678 149 523	100.0	0.442 871 14
0.0125	0.066 702 195 467	125.0	0.449 602 5
0.015	0.068 635 182 797	150.0	0.454 651 1
0.02	0.072 253 547 538	200.0	0.461 821 6
0.025	0.075 581 741 857	250.0	0.466 744 5
0.03	0.078 661 978 338	300.0	0.470 376 2
0.04	0.084 213 203 232	400.0	0.475 440 4
0.05	0.089 120 137 635	500.0	0.478 849 9
0.06	0.093 527 503 781	600.0	0.481 328 1
0.08	0.101 219 398 776	800.0	0.484 727 9
0.1	0.107 812 103 717	1000.0	0.486 977 7
0.125	0.114 953 748 609		
0.15	0.121 195 866 515		
0.2	0.131 784 980 610		
0.25	0.140 614 861 988		
0.3	0.148 221 836 724		
0.4	0.160 923 222 363		
0.5	0.171 342 335 822		
0.6	0.180 205 447 533		
0.8	0.194 790 092 068		

TABLE VIII. Binding energies of the state $3d_{-2}$. The uncertainty of each value is ± 1 in the last digit.

γ	$3d_{-2}$	γ	$3d_{-2}$
1.0×10^{-4}	0.055 705 420 556	1.0	0.353 048 025 149
1.25×10^{-4}	0.055 742 844 619	1.25	0.387 496 964 9
1.5×10^{-4}	0.055 780 251 808	1.5	0.418 078 990 7
2.0×10^{-4}	0.055 855 015 563	2.0	0.471 171 930 7
2.5×10^{-4}	0.055 929 711 824	2.5	0.516 779 036 9
3.0×10^{-4}	0.056 004 340 593	3.0	0.557 151 664 5
4.0×10^{-4}	0.056 153 395 674	4.0	0.627 009 225 2
5.0×10^{-4}	0.056 302 180 844	5.0	0.686 802 520 6
6.0×10^{-4}	0.056 450 696 155	6.0	0.739 581 567 4
8.0×10^{-4}	0.056 746 917 448	8.0	0.830 597 506 3
1.0×10^{-3}	0.057 042 060 175	10.0	0.908 214 775 5
1.25×10^{-3}	0.057 409 473 075	12.5	0.992 449 72
1.5×10^{-3}	0.057 775 203 906	15.0	1.066 511 00
2.0×10^{-3}	0.058 501 629 202	20.0	1.193 633 18
2.5×10^{-3}	0.059 221 359 887	25.0	1.301 491 81
3.0×10^{-3}	0.059 934 426 237	30.0	1.396 028 67
4.0×10^{-3}	0.061 340 717 761	40.0	1.557 699 07
5.0×10^{-3}	0.062 720 864 509	50.0	1.694 321 25
6.0×10^{-3}	0.064 075 310 538	60.0	1.813 683 46
8.0×10^{-3}	0.066 709 218 621	80.0	2.017 032 88
0.01	0.069 247 183 403	100.0	2.188 167 24
0.0125	0.072 292 792 761	125.0	2.371 725 64
0.015	0.075 207 490 379	150.0	2.531 391 02
0.02	0.080 685 874 396	200.0	2.802 000 03
0.025	0.085 758 974 923	250.0	3.028 467 34
0.03	0.090 490 563 102	300.0	3.224 790 43
0.04	0.099 124 530 270	400.0	3.556 212 78
0.05	0.106 888 753 731	500.0	3.832 390 06
0.06	0.113 981 234 765	600.0	4.070 994 26
0.08	0.126 654 630 636	800.0	4.472 201 56
0.1	0.137 839 515 462	1000.0	4.805 110 67
0.125	0.150 315 552 326		
0.15	0.161 543 491 325		
0.2	0.181 320 606 516		
0.25	0.198 555 082 470		
0.3	0.213 976 238 596		
0.4	0.240 982 637 056		
0.5	0.264 389 553 046		
0.6	0.285 253 164 247		
0.8	0.321 640 368 228		

lying energy levels and discuss some general features of the spectrum.

Despite a huge number of various analytical and numerical approaches to the magnetized hydrogen problem, even for the ground state only several values of E_b reported so far have precision better than 10^{-6} hartree [33]. Table I lists the binding energy of the ground state for $10^{-4}\leqslant\gamma\leqslant4\times10^{3}$. The maximal absolute error of each value does not exceed $\pm10^{-12}$ (±1 in the last digits).

Tables II, III, and IV give the binding energies of the states evolving from $2s_0$, $2p_0$, and $2p_{-1}$, respectively. The maximal absolute error of values given in the tables is not higher than ±1 in the last digit. The binding energies of states evolving from $3p_0$, $3p_{-1}$, $3d_{-1}$, and $3d_{-2}$ are presented in Tables V–VIII.

Figures 5(a) and 5(b) show the energy levels of the lowest states with $\nu=0$ and m from 0 to -5 and -10, respectively. It should be realized that these values are valid only in the infinite nuclear mass approximation, since the effect of the finite proton mass renders states with $m\neq0$ unbound if the

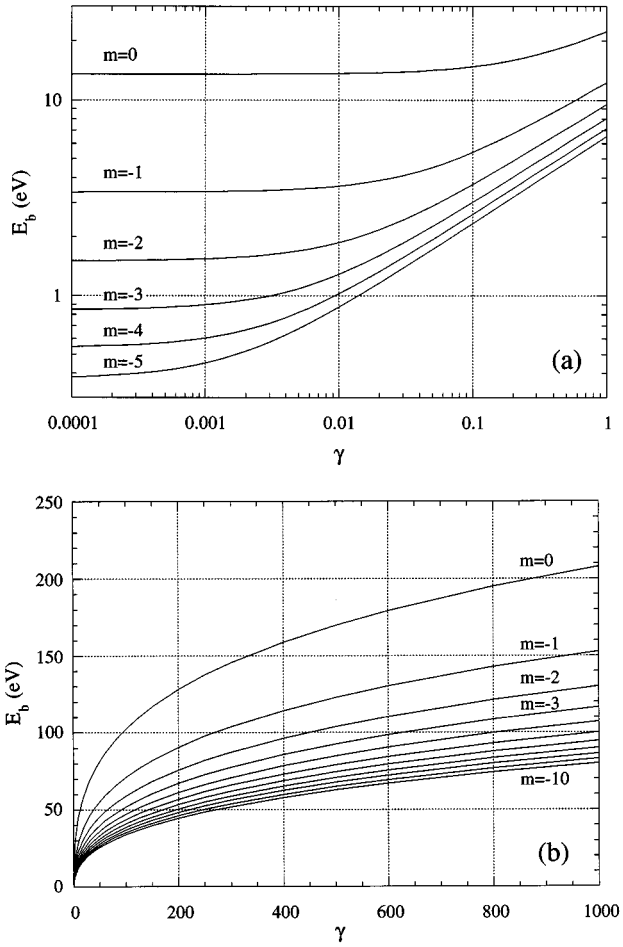

FIG. 5. Evolution of the lowest energy levels with quantum numbers $\nu=0$ and (a) $-5\leqslant m\leqslant 0$, (b) $-10\leqslant m\leqslant 0$.

field is sufficiently large [38]. These figures demonstrate that for large values of γ the energy difference between adjacent levels m and $m+1$ decreases as the magnetic quantum number m increases in magnitude.

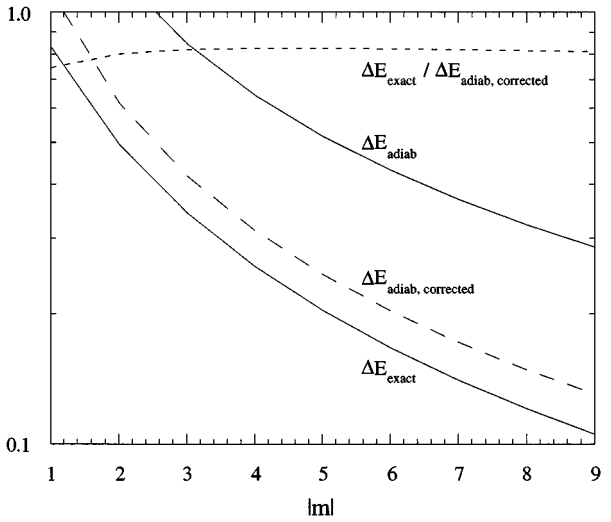

FIG. 6. Comparison of the distance ΔE_{exact} between levels shown in Fig. 5(b) at $\gamma=1000$ with the adiabatic estimates ΔE_{adiab} [Eq. (87)] and $\Delta E_{\text{adiab,corr}}$ [Eq. (88)] (dimensionless units).

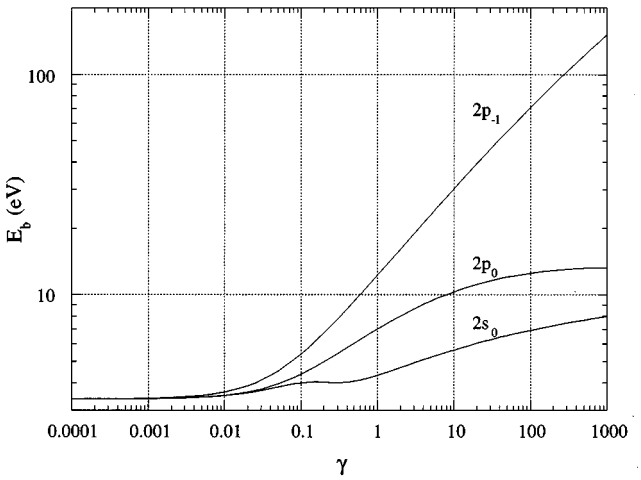

FIG. 7. Dependence of the levels evolving from the field-free states with principal quantum number $n=2$ on the magnetic field γ.

It is interesting to compare the results for large $|m|$ and γ with the predictions of the adiabatic approximation [23]. In the adiabatic approximation the lowest energy level of an atom with quantum numbers $\nu=0$, m is given by

$$(E_{\text{adiab}})_{\nu=0,m}=\frac{1}{2}\ln^2\frac{\gamma}{\sqrt{2|m|+1}}, \tag{86}$$

which is about three times larger than real values, and the energy difference between states with m and $m-1$ is, in the limit of large negative m,

$$\Delta E_{\text{adiab}}=(E_{\text{adiab}})_{\nu=0,m-1}-(E_{\text{adiab}})_{\nu=0,m}$$

$$\approx\frac{1}{2|m|+1}\ln\frac{\gamma}{\sqrt{2|m|+1}},\quad m\to-\infty. \tag{87}$$

Using Eq. (86), the expression for ΔE_{adiab} may be rewritten as

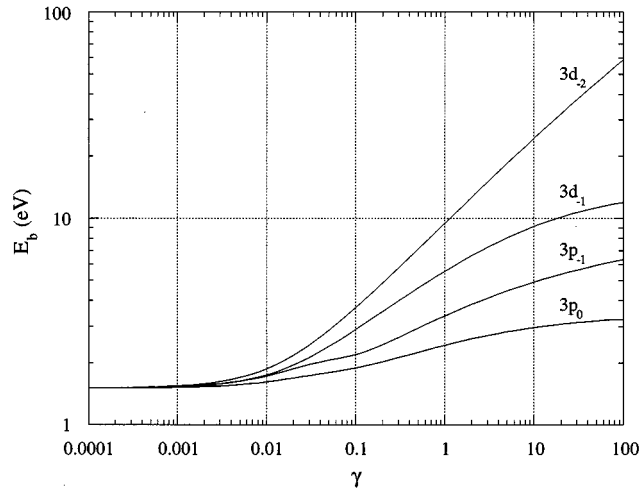

FIG. 8. Evolution of the states $3p_0$, $3p_{-1}$, $3d_{-1}$, and $3d_{-2}$.

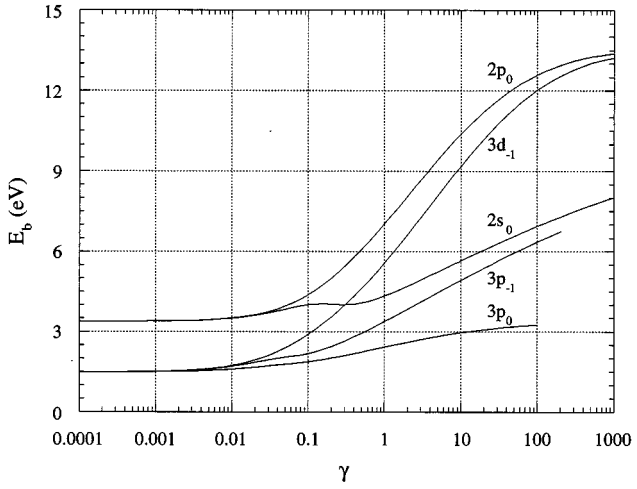

FIG. 9. Behavior of slightly excited levels evolving from field-free states with principal quantum numbers $n=2,3$.

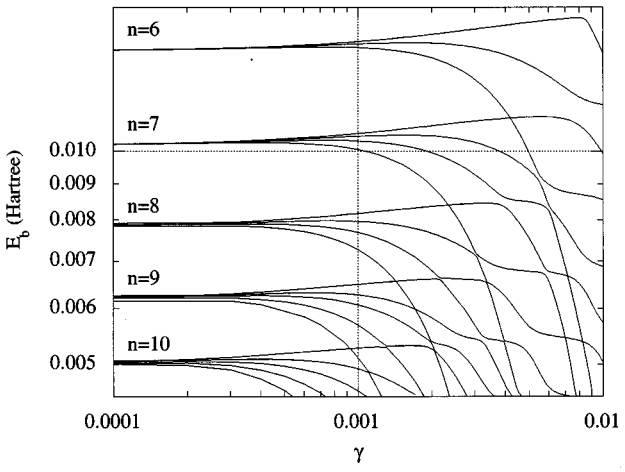

FIG. 10. Irregular behavior of levels with $m=0$, $\pi=+1$ evolving from field-free states with $6\leqslant n\leqslant 10$.

$$\Delta E_{\text{adiab,corr}} \approx \frac{\sqrt{2E_b}}{2|m|+1}, \quad m\to-\infty. \tag{88}$$

The comparison of the exact energy difference between lowest levels ΔE_{exact} with the predictions of the adiabatic approximation (87) and (88) is given in Fig. 6. It is interesting to see that, although ΔE_{adiab} is about three times larger than the exact values ΔE_{exact}, the corrected estimate $\Delta E_{\text{adiab,corr}}$ agrees with the exact values within 20% and, therefore, represents a fair approximation to ΔE_{exact}.

The evolution of levels evolving from the states with main quantum numbers 2 and 3 is shown in Figs. 7 and 8. It is interesting to make a comparison of these two groups of

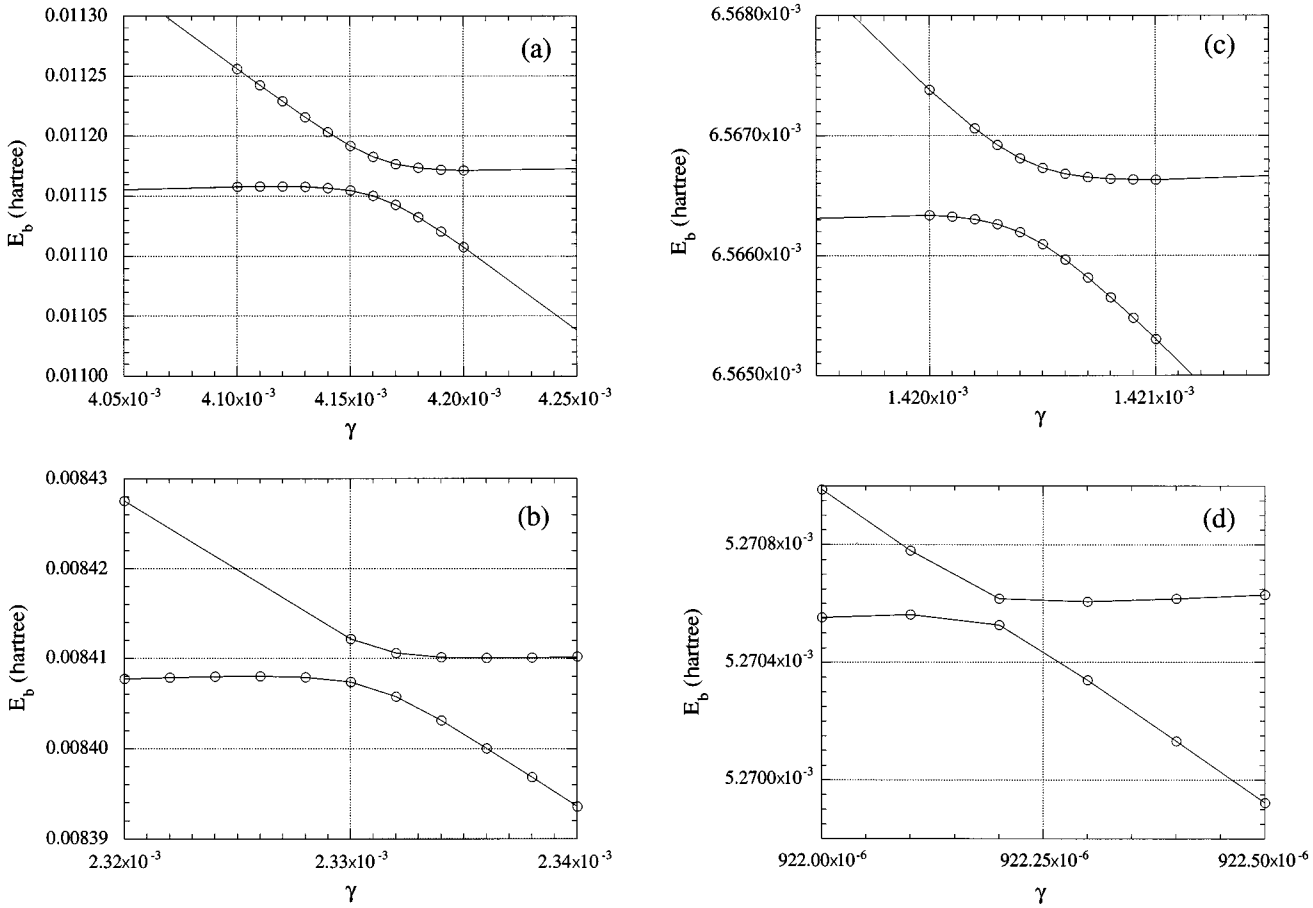

FIG. 11. First avoided crossings between levels with $m=0$ and $\pi=+1$ evolving from field-free states with principal quantum numbers: (a) $n=6$ and $n=7$, (b) $n=7$ and $n=8$, (c) $n=8$ and $n=9$, (d) $n=9$ and $n=10$.

levels. As can be seen from Fig. 9, which shows the curves simultaneously, for large values of γ the levels form groups with the same z parity and number of zeros along the $\theta=0$ axis, but with different m ($2p_0$ and $3d_{-1}$, $2s_0$ and $3p_{-1}$).

Application of the obtained solution to the chaotic region of the spectrum is demonstrated in Figs. 10–12. Figure 10 shows the general picture of levels with $m=0$ and $\pi=+1$ evolving from field-free states with principal quantum numbers $6\leqslant n\leqslant 10$. Anticrossings appearing due to the existence of an approximate constant of motion [15–19] are shown in Figs. 11 and 12. As can be seen in Fig. 11, the width of the first avoided crossings between levels evolving from field-free states with different n decreases exponentially when n increases, while widths of subsequent anticrossings do not exhibit any regular behavior at all, as shown in Fig. 12. This picture strongly suggests that in the well-mixed regime approximate symmetry is substantially lowered.

Along with establishing the exact framework for approximate methods which are being employed for the hydrogen in magnetic field, the data presented in this section demonstrate the large capabilities of the obtained exact solution. Of course, a complete description of the hydrogen spectra requires knowledge not only of several low-lying states but also of many excited states, wavelengths, and oscillator strength. Currently we are working on the compiling of extensive tables of excited states, which will be published in subsequent papers.

VIII. CONCLUSION

We have obtained the exact representation of the solution of the Schrödinger equation describing the hydrogen atom in an external uniform magnetic field. The solution is obtained in the form of a power series in two variables, the radius and the sine of the polar angle. The boundary condition at infinity is reduced to the infinite set of zero-dimensional conditions, and the solution is obtained as the limit of the converging series of reduced solutions.

Therefore, the solution is rigorously defined as an analytical function of two variables. Due to the two-dimensionality of the problem the function is defined as the result of solving an infinite system of equations, in contrast to the usual one-dimensional problems of mathematical physics (e.g., the circular homogeneous vibrating membrane), where eigenvalues are defined implicitly via a single equation (in the membrane example they are zeros of the Bessel functions). Nevertheless, in the strict analogy to the usual special functions of mathematical physics, the solution can be algebraically computed with any desired precision and with exact control over the accuracy of obtained results.

Note that well-known analytical functions, like exponential, hypergeometric functions, etc., are defined as infinite converging series and are exact because their quantitative determination is free of any approximations. Similarly, the solution of the magnetized hydrogen problem is obtained in the form of infinite power series in two variables and its

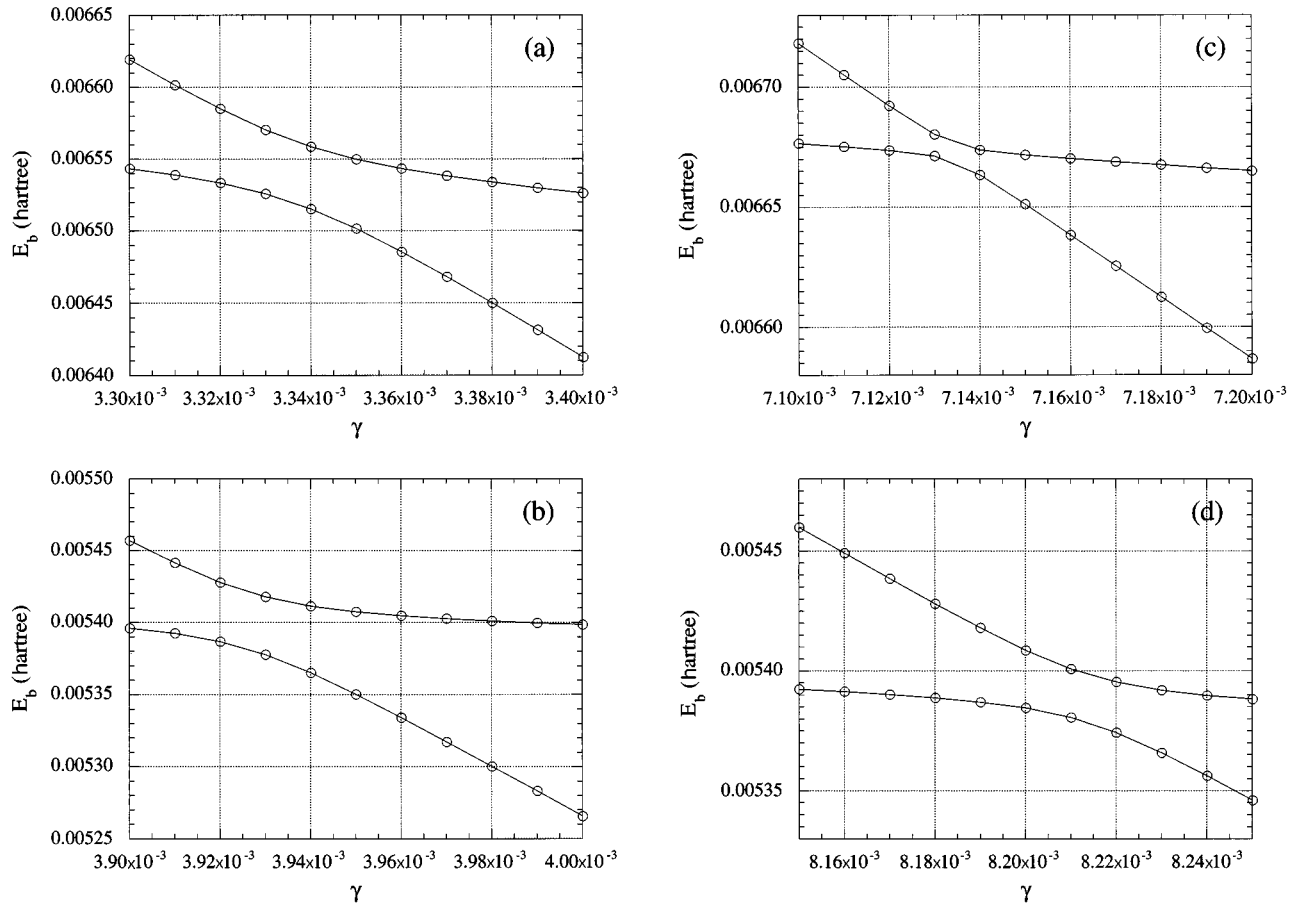

FIG. 12. Four avoided crossings in the region $0.0033<\gamma<0.0085$, $0.53<E_b<0.67$ ($m=0$, $\pi=+1$).

quantitative calculation is free of any approximations inherent to numerical schemes.

It should be specially mentioned that the solution converges perfectly well for all values of magnetic field, from the zero-field limit to the region of ultrahigh fields $\gamma > 1000$, and for any excited states, allowing us to obtain detailed information on the structure of the spectrum in the region of intermediate fields. Although the present work lists only several low-lying states for a widely spaced mesh of γ, we are compiling extensive tables of many quantum states, which are to be published elsewhere.

One should realize that the realistic physical description of the atom requires incorporation of relativistic effects [33], effects of the finite proton mass, which affect transitions between states with different m in strong fields and can even prevent binding for states with nonzero m [38], effects of spin-orbit coupling, and so on. These effects can be obtained as corrections to the exact solution.

The problem of the hydrogen atom in an external magnetic field has important applications in such different research areas as atomic spectroscopy, solid-state physics, and astrophysics. The availability of the exact solution of the problem opens new possibilities for the further development of the theory of matter in ultrahigh magnetic fields. In astronomy, the complete knowledge of the spectrum of the atomic hydrogen in magnetic field, which is now limited only to a small number of low-lying states [8], will help in accurate measurements of stellar magnetic fields. The opportunity to calculate the excited hydrogen energy levels in the chaotic regime is of substantial importance to the investigations of quantum chaos [18]. In addition, the technique presented in the present work has a significant methodological interest and can provide a valuable tool for the solution of other mathematical problems.

ACKNOWLEDGMENTS

This work was supported by the Swedish Natural Research Council (NFR), Contract No. F-AA/FU 10297-307, and by the Swedish Royal Academy, Contract No. 1482.

[1] M. Ruderman, Phys. Rev. Lett. **27**, 1306 (1971).
[2] M. A. Ruderman and P. G. Sutherland, Astrophys. J. **196**, 51 (1975).
[3] J. Arons, Astrophys. J. **266**, 215 (1983).
[4] P. B. Jones, Phys. Rev. Lett. **55**, 1338 (1985).
[5] B. B. Kadomtsev and V. S. Kudryavtsev, Pis'ma Zh. Éksp. Teor. Fiz. **13**, 15 (1971) [JETP Lett. **13**, 9 (1971)].
[6] M. A. Liberman and B. Johansson Usp. Fiz. Nauk **165**, 121 (1995) [Sov. Phys. Usp. **38**, 117 (1995)].
[7] R. Östreicher *et al.*, Astron. Astrophys. **257**, 353 (1992).
[8] H. Ruder, G. Wunner, H. Herold, and F. Geyer, *Atoms in Strong Magnetic Fields* (Springer-Verlag, Berlin, 1994).
[9] R. J. Elliott and R. Loudon, J. Phys. Chem. Solids **15**, 196 (1960).
[10] E. M. Gershenzon, G. N. Gol'tsman, and A. I. Elant'ev, Zh. Éksp. Teor. Fiz. **72**, 1062 (1977) [Sov. Phys. JETP **45**, 555 (1977)].
[11] S. M. Dickmann and D. I. Sidel'nikov, Phys. Lett. **187A**, 79 (1994), and references therein.
[12] A. V. Korolev and M. A. Liberman, Phys. Rev. B **47**, 14 318 (1993); **50**, 14 077 (1994); Phys. Rev. Lett. **72**, 270 (1994).
[13] W. R. S. Garton and F. S. Tomkins, Astrophys. J. **158**, 839 (1969).
[14] J. C. Castro *et al.*, Phys. Rev. Lett. **45**, 1780 (1980).
[15] M. L. Zimmerman, M. M. Kash, and D. Kleppner, Phys. Rev. Lett. **45**, 1092 (1980).
[16] C. W. Clark, Nature (London) **292**, 437 (1981).
[17] C. W. Clark, K. T. Lu, and A. F. Starace, in *Progress in Atomic Spectroscopy*, edited by H. J. Beyer and H. Kleinpoppen (Plenum, New York, 1984), Part C, p. 247.
[18] H. Friedrich and D. Wintgen, Phys. Rep. **183**, 37 (1989), and references therein.
[19] B. D. Simons *et al.*, Phys. Rev. Lett. **71**, 2899 (1993).
[20] L. D. Landau and E. M. Lifshits, *Quantum Mechanics* (Pergamon, Oxford, 1977).
[21] V. D. Krivchenkov and M. A. Liberman, Izv. Vyssh. Uchebn. Zaved. Fiz. **8**, 23 (1968) [Sov. Phys. J. **8**, 45 (1968)].
[22] R. H. Garstang and S. B. Kemic, Astrophys. Space Sci. **31**, 103 (1974).
[23] R. Cohen, J. Lodenquai, and M. Ruderman, Phys. Rev. Lett. **25**, 467 (1970).
[24] A. V. Turbiner, J. Phys. A **17**, 859 (1984).
[25] J. C. Le Guillou and J. Zinn-Justin, Ann. Phys. (N.Y.) **147**, 57 (1983).
[26] W. Rösner, G. Wunner, H. Herold, and H. Ruder, J. Phys. B **17**, 29 (1984).
[27] D. Wintgen and H. Friedrich, J. Phys. B **19**, 991 (1986).
[28] C.-R. Liu and A. F. Starace, Phys. Rev. A **35**, 647 (1987).
[29] C. R. Handy, D. Bessis, G. Sigismondi, and T. D. Morley, Phys. Rev. Lett. **60**, 253 (1988).
[30] P. Falsaperla and G. Fonte, Phys. Rev. A **50**, 3051 (1994), and references therein.
[31] Z. Chen, G. Fonte, and S. P. Goldman, Phys. Rev. A **50**, 3838 (1994).
[32] J. A. C. Gallas, J. Phys. B **18**, 2199 (1985).
[33] S. P. Goldman and Z. Chen, Phys. Rev. Lett. **67**, 1403 (1991); Z. Chen and S. P. Goldman, Phys. Rev. A **44**, 4459 (1991); **45**, 1722 (1992); **48**, 1107 (1993).
[34] U. Kappes and P. Schmelcher, J. Chem. Phys. **100**, 2878 (1994).
[35] J. Shertzer, L. R. Ram-Mohan, and D. Dossa, Phys. Rev. A **40**, 4777 (1989).
[36] O. L. Silva Filho and A. L. A. Fonseca, Phys. Rev. A **50**, 4383 (1994).
[37] H. Herold, H. Ruder, and G. Wunner, J. Phys. B **14**, 751 (1981).
[38] D. Baye and M. Vincke, Phys. Rev. A **42**, 391 (1990), and references therein.